

1 Existence and functions of hypothalamic kisspeptin neuropeptide
2 signaling system in a non-chordate deuterostome species

3

4 Tianming Wang^{1,3*}, Zheng Cao², Zhangfei Shen², Jingwen Yang^{1,3}, Xu Chen¹, Zhen Yang¹, Ke
5 Xu¹, Xiaowei Xiang¹, Qiuhan Yu¹, Yimin Song¹, Weiwei Wang², Yanan Tian², Lina Sun⁴,
6 Libin Zhang^{4,5}, Su tGuo³, Naiming Zhou^{2*}

7

8 ¹National Engineering Research Center of Marine Facilities Aquaculture, Marine Science
9 College, Zhejiang Ocean University, Zhoushan, Zhejiang 316022, People's Republic of China

10 ²Institute of Biochemistry, College of LifeSciences, Zijingang Campus, Zhejiang University,
11 Hangzhou, Zhejiang 310058, People's Republic of China

12 ³Programs in Human Genetics and Biological Sciences, Department of Bioengineering and
13 Therapeutic Sciences, University of California, San Francisco, San Francisco, CA, United
14 States

15 ⁴Key Laboratory of Marine Ecology and Environmental Sciences, Institute of Oceanology,
16 Chinese Academy of Sciences, Qingdao, Shandong 266071, People's Republic of China

17 ⁵Center for Ocean Mega-Science, Chinese Academy of Sciences, Qingdao, Shandong 266071,
18 People's Republic of China

19 These authors contributed equally: Tianming Wang, Zheng Cao and Zhangfei Shen.

20 Correspondence and requests for materials should be addressed to N.Z.

21 (zhounaiming@zju.edu.cn) or to T.W. (wangtianming@zjou.edu.cn)

22

23 **Abstract**

24 The kisspeptin (Kp) system is a central modulator of the hypothalamic-pituitary-gonadal axis
25 in vertebrates. Its existence outside the vertebrate lineage remains largely unknown. Here we
26 report the identification and characterization of Kp system in the sea cucumber *Apostichopus*
27 *japonicus*. The gene encoding the Kp precursor, generates two mature neuropeptides,
28 AjKiss1a and AjKiss1b. The Kp receptors, AjKissR1 and AjKissR2, are strongly activated by
29 synthetic *A. japonicus* and vertebrate Kps, triggering a rapid intracellular mobilization of Ca²⁺,
30 followed by receptor internalization. AjKissR1 and AjKissR2 share similar intracellular
31 signaling pathways via G_{αq}/PLC/PKC/MAPK cascade, when activated by C-terminal
32 decapeptide (AjKiss1b-10). The *A. japonicus* Kp system functions in multiple tissues which
33 are closely related to reproduction and metabolism. Overall, our findings uncover for the first
34 time, to our knowledge, the existence and function of the Kp system in a non-chordate species
35 and provide new evidence to support the ancient origin of the hypothalamic neurosecretory
36 system.

37

38

39 **Introduction**

40 Nervous systems, from simple nerve nets in primitive species to complex architectures in
41 vertebrates, process sensory stimuli and enable animals to generate body-wide responses [1].

42 Neurosecretory centers, one of the major output systems in the animal brain, secrete
43 neuropeptides and nonpeptidergic neuromodulators to regulate developmental and
44 physiological processes [2]. Understanding the evolutionary origin of these centers is an area
45 of active investigation, mostly because of their importance in a range of physical phenomena
46 such as growth, metabolism, or reproduction [3, 4].

47 The hypothalamus constitutes the major part of the ventral diencephalon in vertebrates and
48 acts as a neurosecretory brain center, controlling the secretion of various neuropeptides
49 (hypothalamic neuropeptides) [5, 6]. Outside vertebrates, similar neurosecretory systems have
50 been seen in multiple protostomian species including crustaceans, spiders, and molluscs [7].

51 Specific to echinoderms, which occupy an intermediate phylogenetic position as a
52 deuterostomian invertebrate species with respect to vertebrates and protostomes, increasing
53 evidence, collected from *in silico* identification of hypothalamic neuropeptides and functional
54 characterization of vasopressin/ocytocin (VP/OT)-type signaling system, suggests the
55 existence of a conserved neurosecretory system [4, 8].

56 The hypothalamic neuropeptide kisspeptins (Kps), encoded by the *Kiss1* gene and most
57 notably expressed in the hypothalamus, share a common Arg-Phe-amide motif at their
58 C-termini and belong to the RFamide peptide family [9, 10]. Exogenous administration of
59 Kps triggers an increase in circulating levels of gonadotropin-releasing hormone and
60 gonadotropin in humans, mice, and dogs [11-14]. Accumulating evidence suggests that the Kp

61 system functions as a central modulator of the hypothalamic-pituitary-gonadal (HPG) axis to
62 regulate mammalian puberty and reproduction through a specific receptor, GPR54 (also
63 known as AXOR12 or hOT7T175), which is currently referred to as the Kp receptor (KpR)
64 [15-17]. Following the discovery of Kps and KpRs in mammals, a number of Kp and KpR
65 paralogous genes have been revealed in other vertebrates [18], and a couple of functional
66 Kp/KpR have also been demonstrated in amphioxus [19]. Moreover, Kp-type peptides and
67 their corresponding receptors, in echinoderms, have been annotated *in silico*, based on the
68 analysis of genome and transcriptome sequence data [20-25]. However, to our knowledge,
69 neither the Kp-type peptides nor the corresponding receptors have been experimentally
70 identified and functionally characterized in non-chordate invertebrates. This raises an
71 important question: does the Kp/KpR signaling system have an ancient evolutionary origin or
72 did it evolve *de novo* in the chordate/vertebrate lineages?
73 Here, we addressed this question by searching for Kp/KpR genes in a non-chordate species,
74 the sea cucumber *Apostichopus japonicus*. It is one of the most studied echinoderms and is
75 widely distributed in temperate habitats in the western North Pacific Ocean, being cultivated
76 commercially on a large scale in China [26]. We uncovered *Kiss-like* and *KissR-like* genes by
77 mining published *A. japonicus* data [25, 27], using a bioinformatics approach. Their signaling
78 properties were characterized using an *in vitro* culture system. Through the evaluation of Ca²⁺
79 mobilization and other intracellular signals, we found that *A. japonicus* Kps dramatically
80 activated two Kp receptors (AjKissR1 and AjKissR2), via a GPCR-mediated
81 G_{αq}/PLC/PKC/MAPK signaling pathway, that have functions corresponding to those of the
82 vertebrate Kp system. Finally, we revealed the physiological activities of this signaling

83 system both *in vivo* and *ex vivo*, and we demonstrated the involvement of the Kp system in
84 reproductive and metabolic regulation in *A. japonicus*. Collectively, our findings indicate the
85 existence of a Kp/KpR signaling system in non-chordate deuterostome invertebrates and
86 provide new evidence to support the ancient evolutionary origin of the hypothalamic
87 neurosecretory system [3].

88 **Results**

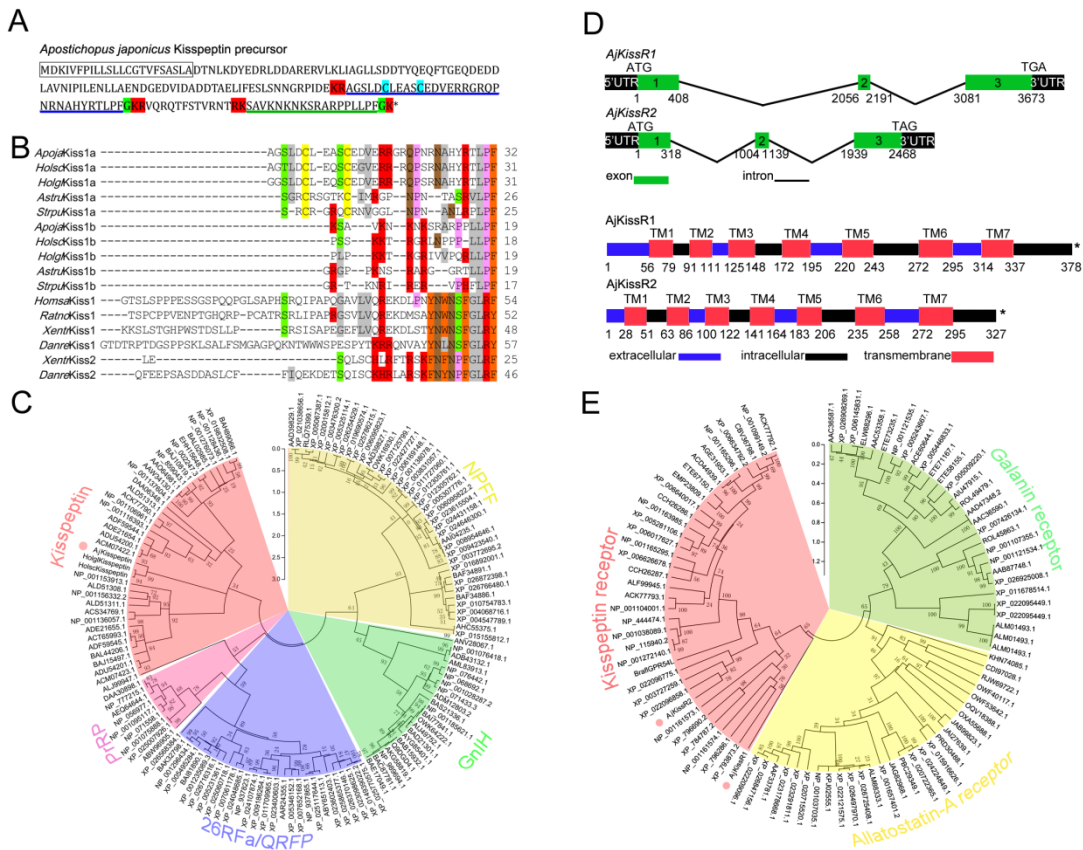
89 ***In silico* identification of Kps and Kp receptors.**

90 Invertebrate Kp receptors have rarely been reported. Putative Kp precursors have been
91 predicted in echinoderms, including starfish (*Asterias rubens*), sea urchin (*Strongylocentrotus*
92 *purpuratus*), and sea cucumbers (*Holothuria scabra*, *Holothuria glaberrima*, and most
93 recently in *A. japonicus*) [22-25]. Based on these sequences, the putative *A. japonicus* Kp
94 precursor gene was identified *in silico* from transcriptome data and cloned from ovarian tissue
95 samples by reverse transcription polymerase chain reaction (RT-PCR). The full-length cDNA
96 (GenBank accession number MH635262) was 2,481 bp long and contained a 543 bp ORF,
97 encoding a 180 amino acid peptide precursor with one predicted signal peptide region and
98 four cleavage sites (Fig. 1A and Figure 1—figure supplement 1). Two mature peptides with
99 amide donors for C-terminal amidation, 32 amino acid Kp-like peptide with a disulfide-bond
100 (AjKiss1a) and 18 amino acid Kp-like peptide (AjKiss1b), were predicted (Supplementary
101 Table 1). Alignment of multiple sequences revealed a high similarity between AjKiss1a/b and
102 predicted echinoderm Kps but low identity between AjKiss1a/b and vertebrate Kiss1/2 (Fig.
103 1B). A maximum likelihood tree of Kp precursors, as well as PrRP, 26RFa/QRFP, GnIH, and
104 NPFF from outgroups [28], was constructed for phylogenetic analysis. It showed that the *A.*

105 *japonicus* Kp precursor, AjKisspeptin, together with kisspeptin-like precursors from the sea
106 cucumbers, *H. scabra* and *H. glaberrima*, were grouped with the vertebrate Kiss1 and Kiss2
107 subfamilies into the ‘Kisspeptin’ group (Fig. 1C).

108 Several predicted ‘G-protein coupled receptor 54-like’ or ‘kisspeptin receptor-like’ gene
109 annotations in the hemichordate *Saccoglossus kowalevskii* (two genes), the echinoderm
110 *Acanthaster planci* (two genes), and *S. purpuratus* (seven genes) have been reported [29-31].
111 Using these predicted genes as reference sequences to search the *A. japonicus* genomic
112 database, three *A. japonicus* Kp receptor-like genes (*AjKissR1*, *AjKissR2*, and *AjKissRL3*;
113 GenBank accession numbers, MH709114, MH709115, and MG199220, respectively) were
114 identified and cloned from *A. japonicus* ovary by RT-PCR. The open reading frames (ORFs)
115 of both *AjKissR1* and *AjKissR2* (detailed data for *AjKissRL3* have not been presented because
116 it exhibited no interaction with ligands in further experiments) comprised three exons, with
117 deduced amino acid sequences of 378 and 327 residues and contained seven transmembrane
118 domains (Fig. 1D and Figure 1–figure supplement 2). A sequence alignment of *AjKissR1* and
119 *AjKissR2*, with the well characterized chordate GPR54, was performed (Figure 1–figure
120 supplement 3) and a relatively high identity in seven transmembrane region sequences,
121 against 21 vertebrate GPR54 sequences was observed, as shown in Figure 1–figure
122 supplement 4. Maximum likelihood phylogenetic tree analysis, using ‘Allatostatin-A receptor’
123 and ‘Galanin receptor’ as outgroups, revealed that *AjKissR1* and 2 both clustered in the
124 “Kisspeptin receptor” group. *AjKissR2* clustered with the predicted *A. planci* (starfish) Kp
125 receptors (Genbank ID: XP_022096858.1 and XP_022096775.1) and with the *S. purpuratus*
126 (sea urchin) Kp receptor (XP_003727259.1), while *AjKissR1* did not group with any known

127 Kp receptors (Fig. 1E).



128

129 **Figure 1.** Gene structure, homology, phylogenetic characterization of *Apostichopus japonicus*
 130 kisspeptin precursor and kisspeptin receptors. **A.** Deduced amino acid sequence of *A. japonicus*
 131 kisspeptin (Kp) precursor. The signal peptide is labeled in box with full lines; the cleavage sites are
 132 highlighted in red; glycine residues responsible for C-terminal amidation are highlighted in green;
 133 cysteines paired in a disulfide-bonding structure are highlighted in light blue; the predicted mature
 134 peptides, AjKiss1a and AjKiss1b, are noted by the blue and green underlines. **B.** Alignment of the
 135 predicted echinoderm Kp core sequences and functionally characterized chordate Kps. Sequences of
 136 *Holothuria scabra*, *Holothuria glaberrima*, *Strongylocentrotus purpuratus*, and *Asterias rubens* Kps
 137 were predicted by Elphick's lab [22, 23]. Vertebrate Kp core sequences were obtained from GenBank
 138 with detailed sequences listed in figure 1 raw data set 1. Color align property was generated using
 139 Sequence Manipulation Suite online. Percentage of sequences that must agree for identity or similarity
 140 coloring was set as 40%. **C.** Phylogenetic tree based on amino acid of kisspeptin precursor and other
 141 four different neuropeptide outgroups [28]. The tree was constructed based on maximum likelihood
 142 algorithms using MEGA 5.1. The detailed sequences are listed in figure 1 raw data set 2. **D.** DNA and
 143 protein structures of AjKissR1/2. *AjKissR1/2* DNA structure is shown with exons numbered in green
 144 bands. ATG represents the start methionine codon and TGA/TAG represents the stop codon.
 145 Organization of the predicted protein structures is shown. The seven transmembrane domains (TM1–
 146 TM7) are marked with red boxes. The N-terminal region and three extracellular (EC) rings are noted
 147 with blue boxes, as well as the C-terminal part and three intracellular (IC) rings are indicated with
 148 black boxes. Stop codons are represented by an asterisk. Arabic numbers under the band indicate the

149 nucleotide or amino acid sites. **E.** Maximum-likelihood trees of kisspeptin (red), allatostatin-A (yellow)
150 and galanin (green) receptors. The tree was constructed by MEGA 5.1 using allatostatin-A and galanin
151 receptors as outgroups [20]. The detailed sequences are listed in figure 1 raw data set 3. The
152 topological stability of these ML trees was achieved by running 1000 bootstrapping replications.
153 Bootstrap values (%) are indicated by numbers at the nodes.

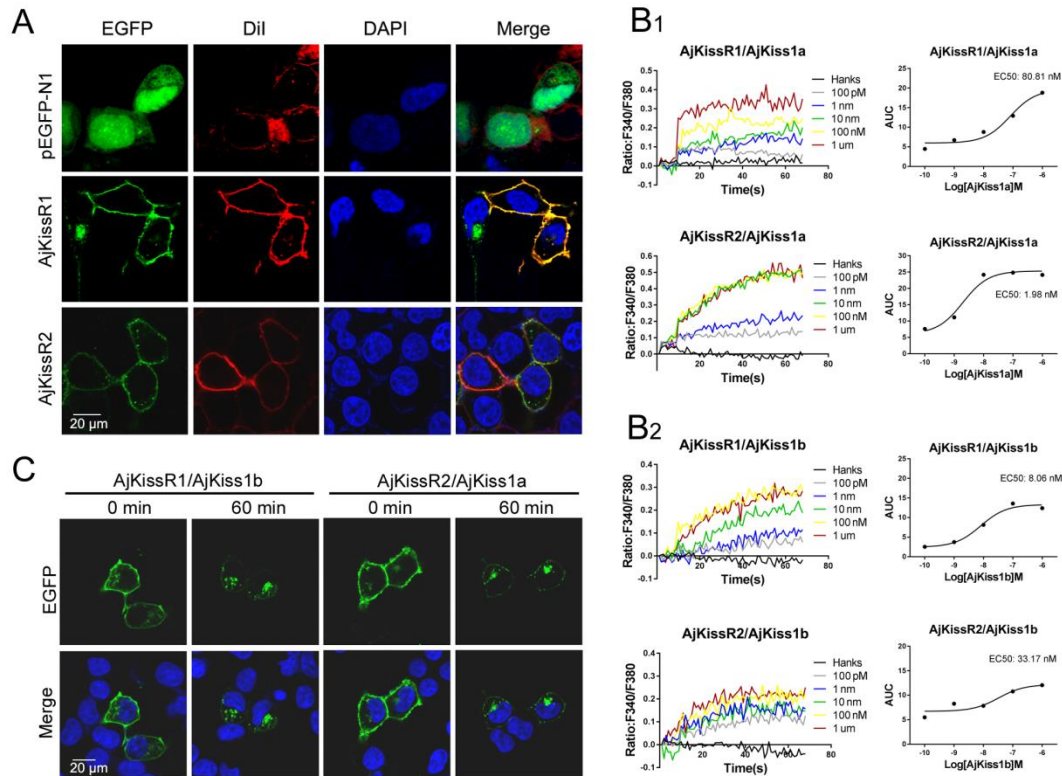
154

155 **Functional expression of putative Kp receptors.**

156 To verify the exact expression and localization of the putative *A. japonicus* Kp receptors,
157 AjKissR1 and 2 with an N-terminal FLAG-tag or with enhanced green fluorescent protein
158 (EGFP) fused to the C-terminal end, were constructed and stably or transiently expressed in
159 human embryonic kidney 293 (HEK293) cells. As shown in Fig. 2A, confocal microscopy
160 revealed that AjKissR1 and 2 were predominantly expressed and localized to the cell surface,
161 with some intracellular accumulation, in the absence of the ligand in HEK293 cells. Next, to
162 examine whether AjKissR1 and AjKissR2 are activated by synthetic Kps, the calcium probe
163 fura-2-based Ca^{2+} mobilization assay was performed. As shown in Fig. 2B, both AjKiss1a and
164 AjKiss1b elicited a rapid increase of intracellular Ca^{2+} , in a concentration-dependent manner,
165 in HEK293 cells transfected with AjKissR1 and AjKissR2, respectively. However, AjKissR1
166 was preferentially activated by AjKiss1b, with an EC50 value of 8.06 nM (Fig. 2B2), whereas
167 AjKissR2 was more specifically activated by AjKiss1a, with an EC50 value of 1.98 nM (Fig.
168 2B1).

169 Agonist-mediated internalization from the cell surface to the cytoplasm has been recognized
170 as a key mechanism in regulating the strength and duration of GPCR-mediated cell signaling
171 and to directly reflect the activation of the receptor [32, 33]. In this study, C-terminal fusion
172 expression of AjKissR1 and 2 with EGFP was used to track the internalization and trafficking
173 of receptors. As shown in Fig. 2C, AjKissR1 and 2 were activated by AjKiss1b and AjKiss1a,

174 respectively, to undergo significant internalization from the plasma membrane to the
 175 cytoplasm. These data provide clear evidence that AjKissR1 and 2 are functional receptors
 176 that are specific for neuropeptides AjKiss1b and AjKiss1a, respectively.



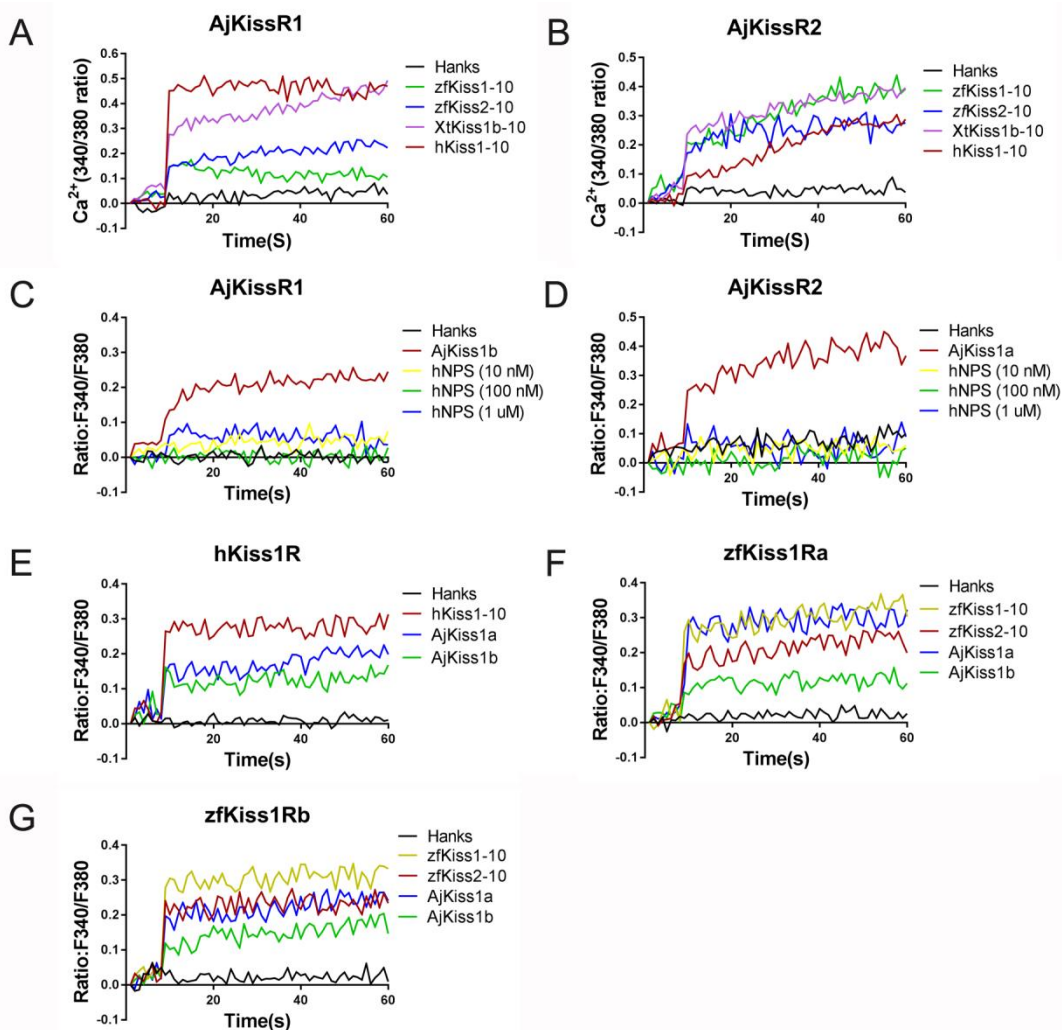
177
 178 **Figure 2.** Functional characteristics of *Apostichopus japonicus* kisspeptins (Kps) and receptors. **A.**
 179 Transiently expressing AjKissR1-EGFP or AjKissR2-EGFP cells were stained with cell membrane
 180 probe (DiI) and cell nucleus probe (DAPI) and detected by confocal microscopy. **B.** Intracellular Ca^{2+}
 181 mobilization in flag-AjKissR1 or flag-AjKissR2 expressing HEK293 cells was measured in response to
 182 indicated concentrations of AjKiss1a (**B1**) and AjKiss1b (**B2**) using Fura-2/AM, with
 183 concentration-dependent course of AjKiss1a or AjKiss1b stimulating Ca^{2+} mobilization in cells. **C.**
 184 Internalization of AjKissR1-EGFP or AjKissR2-EGFP initiated by 1.0 μ M AjKiss1b in stable
 185 AjKissR1-EGFP or 1.0 μ M AjKiss1a in stable AjKissR2-EGFP expressing HEK293 cells determined
 186 after a 60-min incubation by confocal microscopy.

187

188 Ligand selectivity of *A. japonicus* Kp receptors.

189 To examine the cross-reactivity of *A. japonicus* and vertebrate Kp receptors, *A. japonicus*,
 190 human, frog, and zebrafish Kps (hKiss1-10, XtKiss1b-10, zfKiss1-10, and zfKiss2-10) were

191 used to detect their potential in triggering intracellular Ca^{2+} mobilization. As indicated in Fig.
192 2, for AjKissR1, hKiss1-10 and XtKiss1b-10 exhibited higher potency, however, both
193 zfKiss1-10 and zfKiss2-10 showed much lower potency in eliciting Ca^{2+} mobilization (Fig.
194 3A), while for the activation of AjKissR2, XtKiss1b-10, zfKiss1-10, and zfKiss2-10 had a
195 higher potency than hKiss1-10 (Fig. 3B). However, human neuropeptide S (NPS) showed no
196 potency for the activation of both AjKissR1 and AjKissR2 (Fig. 3C and D). Further analysis
197 demonstrated that both AjKiss1a and AjKiss1b could activate hKiss1R, zfKiss1Ra, and
198 zfKiss1Rb with different potency (Fig. 3E, F and G).



199
200 **Figure 3.** Functional cross-talk between the *A. japonicus* and vertebrate Kisspeptin/Kisspeptin receptor
201 systems. Intracellular Ca^{2+} mobilization in AjKissR1 (**A**) or AjKissR2 (**B**) expressing HEK293 cells
202 was measured in response to 1.0 μM zfKiss1-10, zfKiss2-10, XtKiss1b-10, or hKiss1-10 using

203 Fura-2/AM. No Ca^{2+} mobilization-mediated activity was detected in AjKissR1 (C) or AjKissR2 (D)
204 expressing HEK293 cells upon administration of indicated concentrations of human neuropeptide S
205 (hNPS). Intracellular Ca^{2+} mobilization in human kisspeptin (Kp) receptor (hKiss1R) expressing
206 HEK293 cells was measured in response to 1.0 μM hKiss1-10, AjKiss1a or AjKiss1b (E), as well as in
207 zebrafish Kp receptor (zfKiss1Ra or zfKiss1Rb) expressing cells responding to 1.0 μM zfKiss1-10,
208 AjKiss1a, or AjKiss1b (F, G).

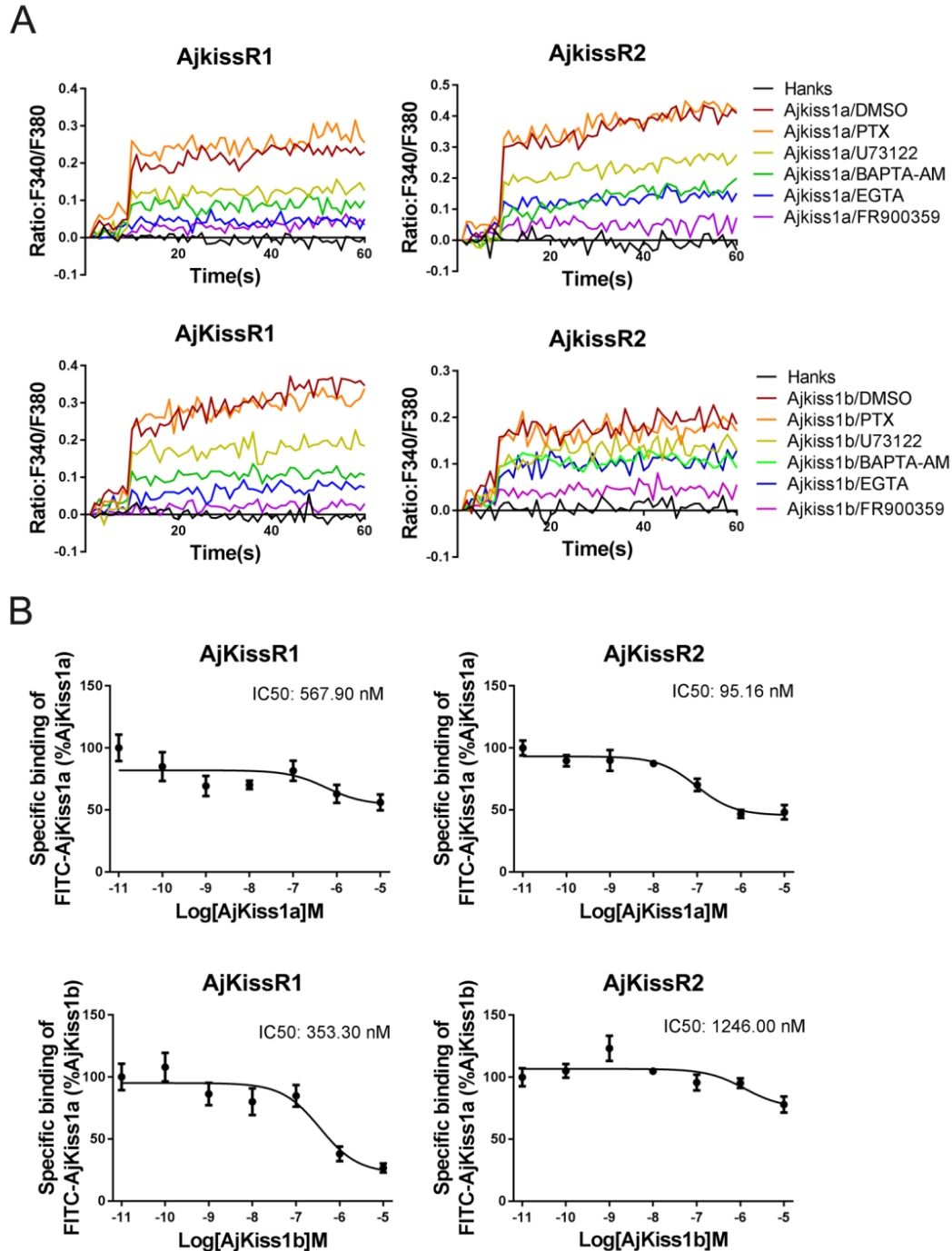
209

210 ***A. japonicus* Kp receptors are directly activated by Kps via a $G_{\alpha q}$ -dependent pathway.**

211 A previous study has demonstrated that in mammals, Kiss1R couples to $G_{\alpha q}$ protein,
212 triggering PLC, intracellular Ca^{2+} mobilization, and the PKC signaling cascade in response to
213 agonists [34]. To elucidate G protein coupling in the activation of both AjKiss1a and
214 AjKiss1b, a combination of functional assays, with different inhibitors, was performed. As
215 shown in Fig. 4A, AjKiss1a and AjKiss1b-eliciting Ca^{2+} mobilization through receptors
216 AjKissR1 and AjKissR2, respectively, were completely blocked by pretreatment with
217 FR900359, a specific inhibitor of $G_{\alpha q}$ protein [35], and also significantly attenuated by PLC
218 inhibitor U73122, extracellular calcium chelator EGTA, and intracellular calcium chelator
219 1,2-bis(o-aminophenoxy)ethane N,N,N',N'-tetraacetic acid acetoxymethyl ester (BAPTA-AM)
220 [36].

221 Next, a competitive binding assay was established by using a synthesized FITC-tagged
222 AjKiss1a at the N-terminus (FITC-AjKiss1a), for assessing the direct interaction of AjKissR1
223 and AjKissR2 with AjKiss1a and AjKiss1b. Functional assays revealed that FITC-AjKiss1a
224 exhibited the potential to induce Ca^{2+} mobilization comparable to the wild-type neuropeptide
225 (Figure 4–figure supplement 1). The competitive displacement of FITC-AjKiss1a with
226 AjKiss1a and AjKiss1b in HEK293/AjKissR1 and AjKissR2 cells was measured by FACS
227 (Fluorescent Activated Cell Sorting) analysis. As shown in Fig. 4B, unlabeled AjKiss1a and

228 AjKiss1b were found to compete with FITC-labeled AjKiss1a with IC₅₀ values of 95.16 and
 229 353.30 nM in AjKissR2 and AjKissR1-transfected HEK293 cells, respectively.



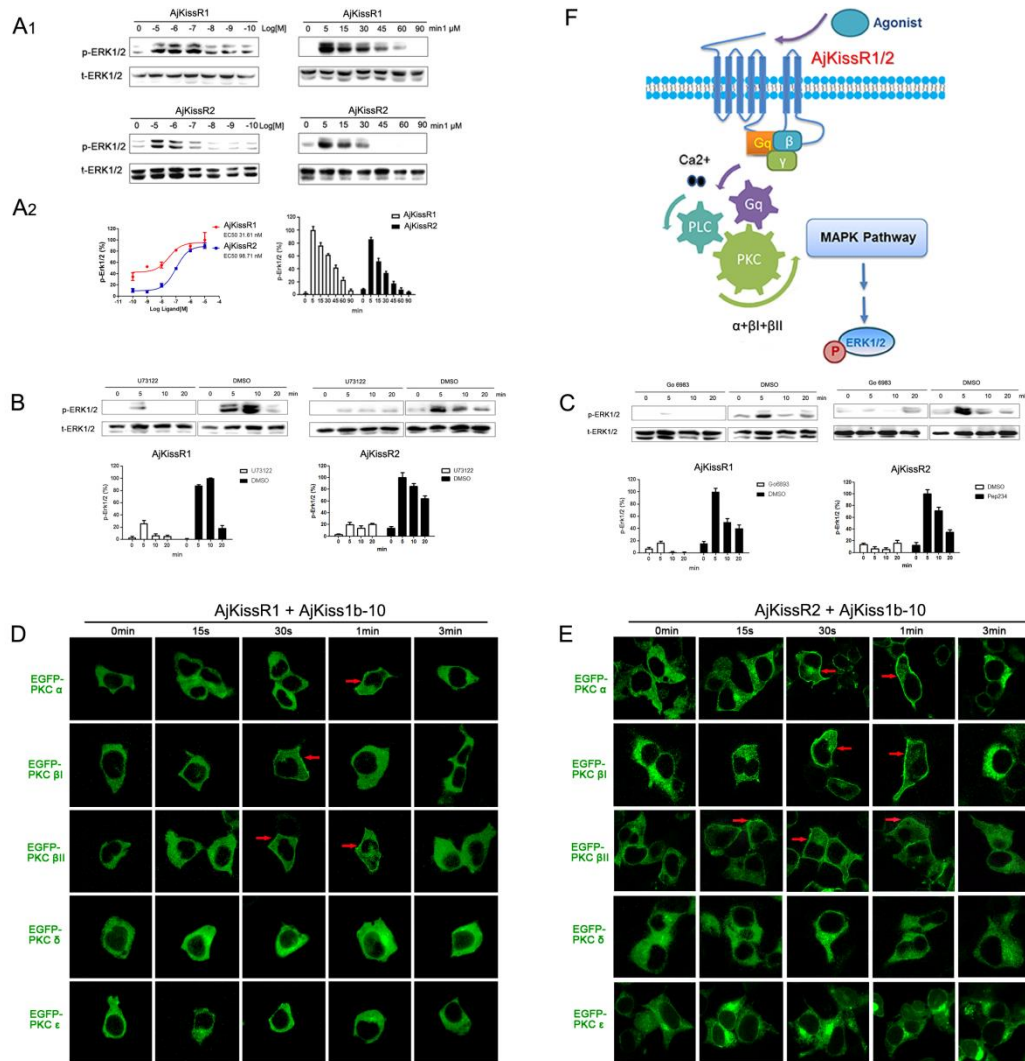
230
 231 **Figure 4.** *Apostichopus japonicus* kisspeptin (Kp) receptors are directly activated by Kps via a
 232 G_{αq}-dependent pathway. **A.** Intracellular Ca²⁺ mobilization in AjKissR1 and AjKissR2 expressing
 233 HEK293 cells was measured in response to 100 nM AjKiss1a or AjKiss1b pretreated with DMSO, G_{αq}
 234 protein inhibitor (FR900359, 1.0 μM), PLC inhibitor (U73122, 1.0 μM), intracellular calcium chelator

235 (BAPTA-AM, 100.0 μ M), or extracellular calcium chelator (EGTA, 5.0 mM). **B.** Competitive binding
236 of 1.0 μ M FITC-AjKiss1a to AjKissR1 or AjKissR2 in the presence of the indicated concentration of
237 AjKiss1a or AjKiss1b. Error bars represent the SEM for 3 independent experiments.

238

239 **AjKissR1 and AjKissR2 are activated by AjKiss1b-10 and signal through the**
240 **G_{αq}-dependent MAPK pathway.**

241 Since AjKiss1b-10 exhibited high potency to activate both AjKissR1 and AjKissR2 in
242 HEK293 cells (Figure 5–figure supplement 1), it was used to conduct further *in vitro* and *in*
243 *vivo* experiments. The previous results reveal that the AjKissR1 and AjKissR2 can be
244 activated by ligands and signals through G_{αq}-dependent Ca²⁺ mobilization; however, the
245 detailed signaling pathway remained to be elucidated. To address this and to evaluate
246 AjKissR1 and AjKissR2 mediated signaling pathway, different inhibitors were used to test
247 intracellular ERK1/2 activation in 293 cells, expressing AjKissR1 and AjKissR2, treated with
248 Ajkiss1b-10. As shown in Fig. 5A, stimulation with AjKiss1b-10, led to the activation of both
249 AjKissR1 and AjKissR2, inducing significant ERK1/2 activation. Further assessment
250 demonstrated that AjKissR1 or AjKissR2-mediated activation of ERK1/2 was significantly
251 blocked by the PLC inhibitor, u73122 (10 μ M), and the PKC inhibitor, Gö6983 (1 μ M) (Fig.
252 5B and C). Moreover, we determined that PKC α , PKC β I, and PKC β II are involved in the
253 activation of the MAPK pathway, using a PKC subtype recruitment assay (Fig. 5D and E).
254 Overall, these results suggest that AjKissR1 and AjKissR2, once activated by ligand, can
255 activate the MAPK cascade, particularly ERK1/2, via the G_{αq}/PLC/PKC signaling pathway
256 (Fig. 5F).



257
 258 **Figure 5.** Cell signaling pathway mediated by AjKissR1 or AjKissR2. **A.** Concentration-dependence
 259 and time course of AjKiss1b-10 stimulated phosphorylation of ERK1/2 in stable FLAG-AjKissR1 or
 260 FLAG-AjKissR2-expressing HEK293 cells, which were incubated with indicated concentrations or
 261 times. **B-C.** ERK1/2 phosphorylation, mediated by AjKiss1b-10, was blocked in FLAG-AjKissR1 or
 262 FLAG-AjKissR2-expressing HEK293 cells, pretreated with PLC or PKC inhibitor. Serum-starved
 263 HEK293 cells were pretreated with DMSO, PLC inhibitor (U73122, 10 μM), or PKC inhibitor
 264 (Gö6983, 10 μM). **D-E.** Role of various PKC isoforms in the activated signaling pathways of sea
 265 cucumber kisspeptin receptor. HEK293 cells, co-transfected with FLAG-AjKissR1 or FLAG-AjKissR2
 266 and different EGFP-PKC isoforms, were stimulated by 1 μM AjKiss1b-10 for the indicated time and
 267 then examined by confocal microscopy. Red arrows denote the recruitment of EGFP-PKC isoforms on
 268 cell membrane. **F.** Schematic diagram of agonist-induced *A. japonicus* kisspeptin receptor activation.
 269 AjKiss1b-10 binding to AjKissR1 or AjKissR2 activates G_{αq} family of heterotrimeric G protein, which
 270 leads to dissociation of the G protein subunits Gβγ, and activates PLC, leading to intracellular Ca²⁺
 271 mobilization, which activates PKC (isoform α and β) and stimulates phosphorylation of ERK1/2. The
 272 p-ERK1/2 was normalized to a t-ERK1/2. Error bars represent SEM for 3 independent experiments.

273

274 **Physiological functions of the Kp signaling system in *A. japonicus*.**

275 To further assess the physiological roles of the Kp signaling system in *A. japonicus*, we
276 examined the tissue distribution of *A. japonicus* Kp/KpR, using custom rabbit polyclonal
277 antibodies for *A. japonicus* kisspeptin precursor and AjKissR1. Tissue-specific western blot
278 analysis revealed the expression of the kisspeptin precursor in the respiratory tree (RET),
279 ovary (OVA), testis (TES), and anterior part (ANP, containing nerve ring as shown in Figure
280 6–figure supplement 1E, F) of mature sea cucumbers (maturity of gonads was evaluated by
281 H&E staining, as shown in Figure 6–figure supplement 1B). AjKissR1 was detected in the
282 RET, OVA, ANP, and muscle (MUS) (Fig. 6A). To reveal the *in situ* distribution of the
283 kisspeptin precursor and receptor, we performed immunofluorescence labeling on tissue
284 sections. Consistent with results from the western blot assay, significant expression of the
285 kisspeptin precursor was observed in the RET, TES, and nerve ring in ANP sections, with no
286 expression in the OVA and MUS; AjKissR1 expression was observed in the RET, OVA, MUS
287 and nerve ring in ANP sections, with rare expression in TES (Fig. 6B). At the cellular level,
288 the kisspeptin precursor was mainly detected in the coelomic epithelium of RET, while the
289 AjKissR1 was detected in the brown bodies, which can be found in luminal spaces of RET
290 and might be related with foreign material removal [37]. In particular, significant expression
291 and cell membrane localization of AjKissR1 was detected in oocytes, indicating the consistent
292 molecular property of AjKissR1 *in vivo* and *in vitro*. From the TES sections, significant
293 fluorescence signal of the kisspeptin precursor, while a weak signal of AjKissR1, can be
294 detected in spermatogenic epithelium. Significant expression of AjKissR1 was detected in the
295 epithelium of muscle from MUS sections. Moreover, from the ANP sections, the kisspeptin

296 precursor was detectable in the outer surface part of nerve ring (mainly containing the cell
297 body of neurons, as shown in Figure 6–figure supplement 1F2), while the AjKissR1 was
298 detected in the internal region of nerve ring (mainly containing axon of neurons, as shown in
299 Figure 6–figure supplement 1F2).

300 To verify the physiological function of *A. japonicus* kisspeptins, cultured oocytes were
301 stimulated by different Kps. As shown in Fig. 6C, significant ERK phosphorylation signal can
302 be detected by western blot assay in different Kp-treated oocytes that can be blocked by
303 kisspeptin antagonist pep234 (1 μ M) in zfKiss1-10 or AjKiss1b-10 administrated cells
304 (inhibitory effect of pep234 was preapproved *in vitro* as shown in Figure 6–figure supplement
305 2). Further detection of the pERK signal in AjKiss1b-10 treated oocytes by confocal
306 microscopy demonstrated the physiological activation of this pathway by AjKiss1b-10 and
307 pep234 on *A. japonicus* cells (Fig. 6D).

308 Based on the confirmation of their functional activity in cultured oocytes, AjKiss1b-10 and
309 pep234 were used to conduct further *in vivo* experiments. Sea cucumbers treated with
310 AjKiss1b-10 for 40 days exhibited weight loss ($p=0.0583$, Tukey's multiple comparison test, as
311 shown in Fig. 6E) and extremely significant intestinal degeneration ($p=0.0001$, Tukey's multiple
312 comparison test, as shown in Fig. 6F, G), which are the characteristic phenotypes of aestivating
313 *A. japonicus* [38]. Moreover, extremely significant elevation of pyruvate kinase PK
314 transcription ($p=0.0001$, Tukey's multiple comparison test, as shown in Figure 6–figure
315 supplement 3A), which is the rate-limiting enzyme in the regulation of glycolysis and
316 metabolic depression in aestivating *A. japonicus* [39], was detected in the respiratory tree,
317 while a significant decrease of PK transcription was found in muscle ($p=0.0497$, Tukey's

318 multiple comparison test, as shown in Figure 6–figure supplement 3A). To evaluate the potential
319 role of AjKiss1b-10 in regulating reproductive activity, we examined the estradiol (E2) levels
320 in the coelomic fluid of sea cucumber; however, no significant difference was observed in
321 animals treated with AjKiss1b-10 (Figure 6–figure supplement 3B).

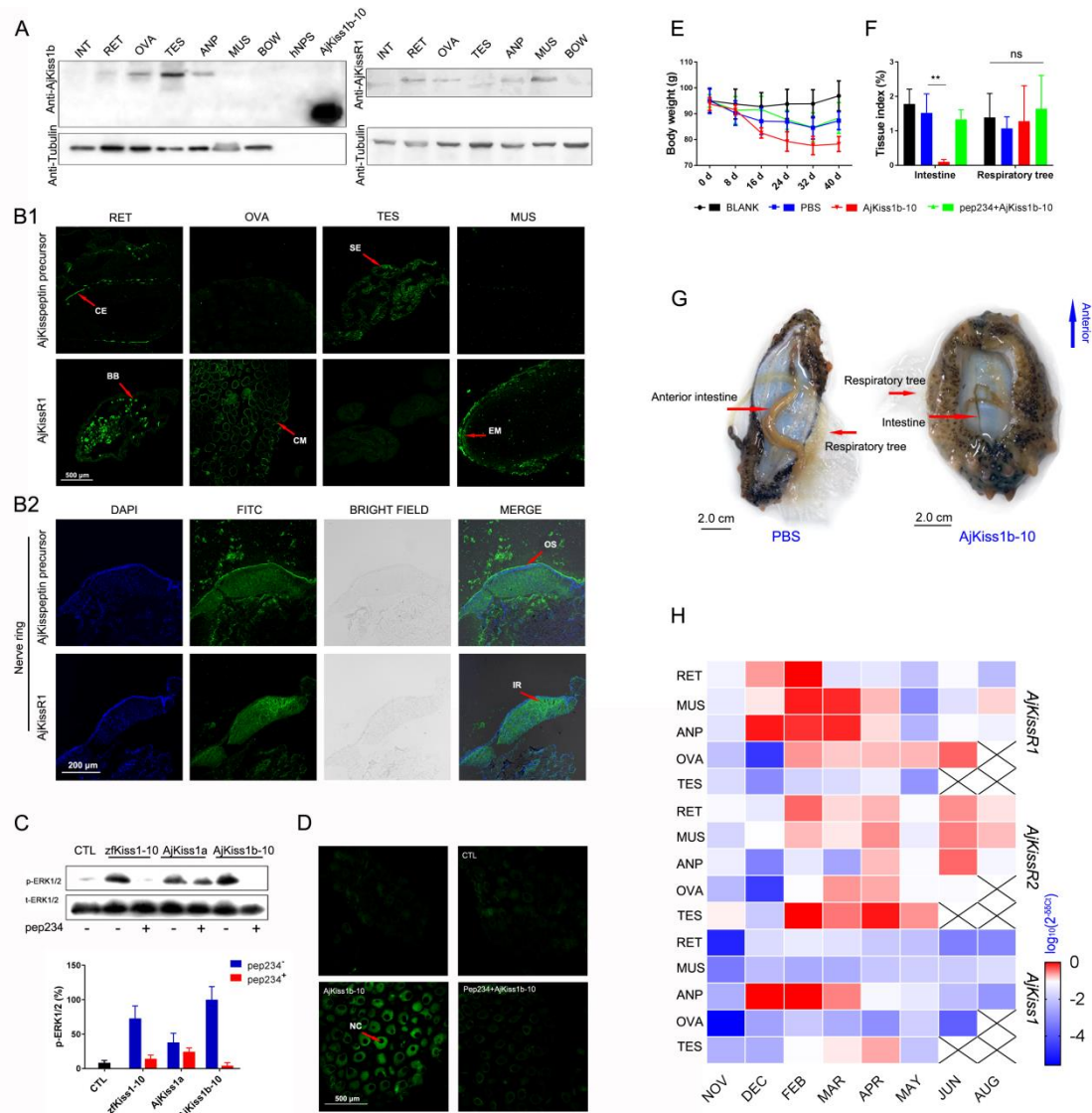
322 The transcriptional expressions of the *A. japonicus* Kp precursor (*AjKiss1*) and Kp receptors
323 (*AjKissR1/2*) were investigated at different stages of reproductive development using the
324 qPCR method. Two-year old sea cucumbers, with 85.29 ± 9.47 g body weight (Figure 6–
325 figure supplement 4A), were collected and various tissues were sampled for further analysis.

326 As shown in Figure 6–figure supplement 4B, notable changes in the relative gut mass and the
327 relative ovary weight of sea cucumber were detected in the developing reproductive stage
328 from November to April, mature reproductive stage in May, after spawning in June, and
329 during aestivation in August. At all stages, *AjKissR1/2* expression was detectable in the

330 majority of sea cucumber tissues, especially after February (Fig. 6H), while significant
331 expression of *AjKiss1* was found in the ANP from December to April with a peak value
332 detected in February. Taken together, the high expression levels of *A. japonicus* Kp precursor
333 mRNA during reproductive development suggests its role in the regulation of reproduction,

334 while the wide distribution of *AjKissR1* and *AjKissR2*, in the other tissues investigated,
335 indicates diverse functions for these two receptors.

336



337

338 **Figure 6.** Physiological function analysis of Kp/KpR signaling systems in *Apostichopus japonicus*. **A.**
 339 Western Blot analysis of *A. japonicus* kisspeptin precursor and AjKissR1 in different tissues of sea
 340 cucumber. (INT) intestine, (RET) respiratory tree, (ANP) anterior part, (OVA) ovary, (TES) testis,
 341 (MUS) muscle, and (BOW) body wall. **B.** Immunofluorescence histochemical staining of *A. japonicus*
 342 kisspeptin precursor and AjKissR1 in RET, OVA, TES, MUS (B1) and nerve ring (B2) of the sea
 343 cucumber. (CE) coelomic epithelium, (BB) brown body, (CM) cell membrane, (SE) spermatogenic
 344 epithelium, (EM) epithelium of muscle, (OS) outer surface, (IR) internal region. **C.** ERK1/2
 345 phosphorylation activity of Kps and inhibitory effect of pep234 on the cultured ovary of sea cucumber.
 346 Samples were evaluated after 2 h of ligand administration, with or without a 4 h pretreatment of
 347 pep234, in optimized L15 medium at 18 °C. Error bars represent SEM for 3 independent experiments.
 348 **D.** Immunofluorescence histochemical staining of pERK signal in cultured oocytes of sea cucumber.
 349 Samples were collected and fixed after 2 h of ligand administration with or without a 4 h pretreatment
 350 of pep234, in optimized L15 medium at 18 °C. NC indicates nucleus of oocytes. **E–F.** Variation of
 351 body weight (**E**) and tissue index (**F**) over 40 days of stimuli treatment. Each symbol and vertical bar
 352 represent SEM (n=5). * indicates significant differences (P < 0.05) and ** indicates extremely
 353 significant differences (P < 0.01), ANOVA, Tukey's multiple comparison test. **G.** Degenerated intestine

354 in AjKiss1b-10 treated sea cucumbers. **H.** Heatmap showing the expression profile of *A. japonicus*
355 kisspeptin and kisspeptin receptors (*AjKissR1/R2* and *AjKiss1*) in different tissues and developmental
356 stages of sea cucumber. The variation in color represents the relative expression level of each gene in
357 different samples (normalized against the peak values in all samples and logarithmized). The number of
358 tissues used for all samples is six, except for the number of ovary samples, with one in NOV
359 (November) and JUN (June), three in DEC (December) and FEB (February), five in MAR (March),
360 and six in APR (April) and MAY (May), and in testis, with two in NOV (November) and DEC
361 (December), four in FEB (February) and MAR (March), and six in APR (April) and MAY (May).

362

363 **Discussion**

364 The functional characterization of neuropeptides or secretory neurons of non-vertebrates
365 contributes to our understanding of the evolutionary origin and conserved roles of the
366 neurosecretory system in animals, especially in Ambulacrarians (deuterostomian invertebrates
367 including hemichordates and echinoderms), which are closely related to chordates [3, 8]. The
368 hypothalamic neuropeptide kisspeptin (Kp), acts as a neurohormone and plays important roles
369 in the regulation of diverse physiological processes in vertebrates, including reproductive
370 development [40, 41], metastasis suppression [42], metabolism and development [43-45],
371 behavioral and emotional control [46], and the innate immune response [47].

372 Though a functional Kp/KpR system has been demonstrated in the chordate amphioxus and a
373 number of invertebrate Kp/KpR genes have been predicted recently, missing experimental
374 identification of a Kp-type system in non-chordates makes it difficult to determine if this
375 signaling system has an ancient evolutionary origin in invertebrates or if it evolved *de novo* in
376 the chordate/vertebrate lineages. In this study, two Kp receptors from the sea cucumber *A.*
377 *japonicus*, AjKissR1 and AjKissR2, have been established to have a high affinity for
378 synthetic Kps from *A. japonicus* or vertebrates and to share similar intracellular signaling, via
379 the $G_{\alpha q}$ /PLC/PKC/MAPK pathway. Results from the *in vivo* investigation indicate that the

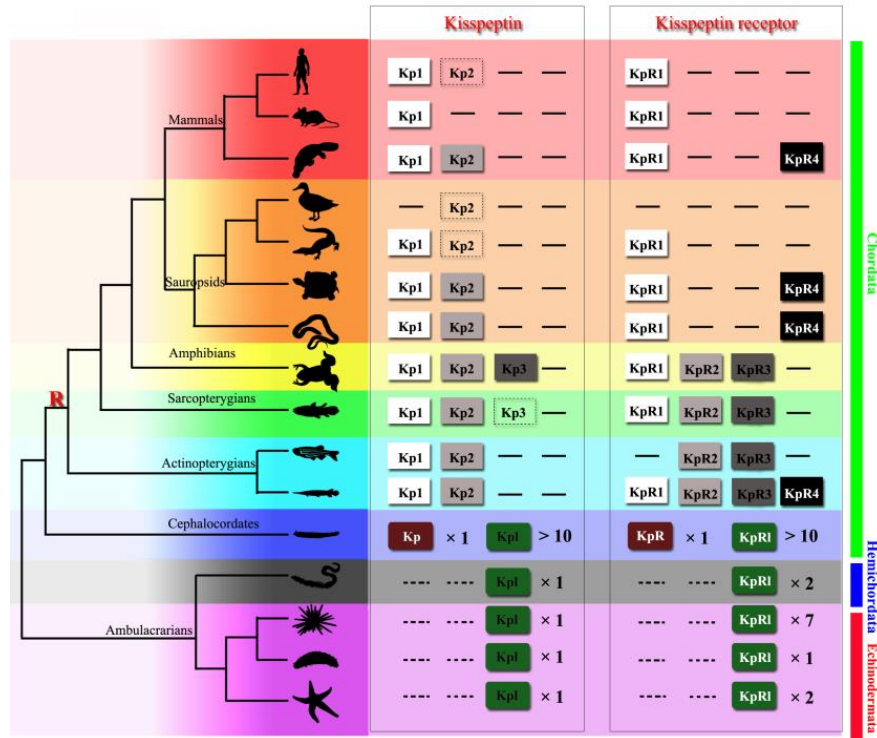
380 Kp/KpR system in sea cucumber might be involved in both metabolic and reproductive
381 control. Given the highly conserved intracellular signaling pathway and physiological
382 functions revealed for the *A. japonicus* Kp/KpR system, it is interesting to speculate that Kp
383 signaling might have originated from non-chordate invertebrates.

384 **Two putative Kp receptors can be activated by multiple synthetic Kp-type peptides in *A.***
385 ***japonicus***

386 Kps or KpRs in Chordata have been functionally recognized in various species. Virtual
387 screening of the transcriptome and genome sequence data for neuropeptide precursors has
388 made a great contribution to Kp/KpR paralogous gene prediction in Ambulacrarians and
389 provides valuable information for further investigation (Fig. 7). In 2013, Kp-type receptors
390 were first annotated in the genome of the acorn worm (*S. kowalevskii*) and purple sea urchin
391 (*S. purpuratus*) [20, 48]. Moreover, a Kp-type neuropeptide precursor with 149-amino acid
392 residues was identified in the starfish *A. rubens*, comprising two putative Kp-type peptides,
393 ArKp1 and ArKp2 [24]. Subsequently, *in silico* analysis of neural and gonadal transcriptomes
394 enabled the virtual discovery of Kps in the sea cucumbers *H. scabra* and *H. glaberrima* [23].
395 Moreover, the presence of Kps in extracts of radial nerve cords was confirmed by proteomic
396 mass spectrometry in the crown-of-thorns starfish *A. planci* [49]. Recently, a 180-residue
397 protein comprising two putative Kp-type peptides has been predicted and a C-terminally
398 amidated peptide GRQPNRNAHYRTLPH-NH₂ was confirmed by mass spectrometric
399 analysis of control nerve ring extracts [25]. These advances provide a basis for experimental
400 studies on the Kp/KpR system in echinoderms.

401 In the present study, we cloned the full length of *Kiss* cDNA sequence from the nerve ring,

402 encoding a putative Kp precursor, which has been predicted from the proteomic analysis of *A.*
403 *japonicas* [25] and synthesized the peptides AjKiss1a (32aa), AjKiss1a-15, AjKiss1a-13,
404 AjKiss1a-10, AjKiss1a (18aa), and AjKiss1b-10, for further experimental tests. Two candidate
405 *A. japonicus* Kp receptors were screened from genomic data, based on the sequence of the
406 identified kisspeptin receptors [19, 20, 29-31, 48, 50] and functionally characterized. Our data
407 shows that despite a low percentage homology between AjKissR1 and 2, synthetic *A.*
408 *japonicus* Kp peptides (AjKiss1a and AjKiss1b) could activate both the receptors, thereby
409 initiating significant receptor internalization and extensive Ca²⁺ mobilization, albeit with a
410 different potency. This is consistent with previous studies demonstrating that in
411 non-mammalian species, synthetic Kiss1 and Kiss2 activated Kp receptors *in vitro* with
412 differential ligand selectivity [51, 52]. In particular, the truncated peptide AjKiss1b-10
413 demonstrated high activity to elicit intracellular Ca²⁺ mobilization in AjKissR1/2 expressing
414 HEK293 cells, while the truncated peptides, AjKiss1a-15, AjKiss1a-13, and AjKiss1a-10,
415 failed to activate the receptors. The functional activity of the truncated peptide AjKiss1b-10 is
416 not unusual, considering that alternative cleavage occurs in the Kps of vertebrates [51, 53];
417 however, the inactivity of AjKiss1a-15, which was identified from mass spectrometric
418 detection in *A. japonicus* [25], raised more questions about the functional and structural
419 characteristics of this neuropeptide and requires further investigation.



420

421 **Figure 7.** Recently identified Kisspeptin (Kp) or Kisspeptin receptor (KpR) genes among some
 422 deuterostomes. The species, indicated by silhouette images downloaded from the *PhyloPic*
 423 database, were clustered in a phylogenetic tree and classified by different colors. Red highlighted “R” indicates a
 424 whole-genome duplication event. Kp/KpR indicates the identified Kisspeptin/Kisspeptin receptor gene,
 425 and Kp1/KpR1 indicates predicted Kisspeptin-like/Kisspeptin-like receptor gene. Dashed boxes denote
 426 symbols indicate pseudogenes. Arabic numerals indicate the number of genes identified or predicted
 427 from public data. The evolutionary tree of indicated species was modified from Pasquier et al. 2014
 428 [18]. Image credits: All silhouettes from PhyloPic, human by T. Michael Keeseyacorn; mouse by
 429 Anthony Caravaggi; platypus by Sarah Werning; duck by Sharon Wegner-Larsen; crocodile by B
 430 Kimmel; turtle by Roberto D áz Sibaja; python by V. Deepak; frog uncredited; coelacanth by Yan
 431 Wong; zebra fish by Jake Warner; spotted gar by Milton Tan; Branchiostoma by Mali'o Kodis,
 432 photograph by Hans Hillewaert; acorn worm by Mali'o Kodis, drawing by Manvir Singh; starfish by
 433 Hans Hillewaert and T. Michael Keesey; sea cucumber by Lauren Sumner-Rooney; sea urchin by Jake
 434 Warner;

435

436 **Cross interaction between *A. japonicus* and the Kp/KpR systems of vertebrates**
 437 **confirmed the existence of Kp signaling systems in Echinoderm**

438 In the mammalian genome, a single *Kiss1* gene produces a mature 54-amino acid peptide,
 439 Kp-54, which is further proteolytically truncated to 14 and 13 amino acid carboxyl-terminal
 440 peptides, Kp-14 and Kp-13, with a common C-terminal decapeptide (Kp-10) core [53, 54]. In

441 non-mammalian vertebrates, two paralogous Kp genes, *Kiss1* and *Kiss2*, are present in the
442 genome of teleosts, producing two mature peptides, which share the highly conserved Kp-10
443 region with mammalian Kps [50, 51, 55]. Unlike mammalian and non-mammalian vertebrates,
444 in the sea cucumber *A. japonicas*, only one Kp gene was annotated and isolated. However,
445 sequence analysis revealed that the Kp gene encodes a 180 amino acid peptide precursor,
446 which is proteolytically cleaved to two mature peptides, consistent with other KPs identified
447 in the phylum Echinodermata [22, 24, 49]. Both putative mature peptides have a C-terminal
448 Leu-Pro-Phe-amide motif, instead of the Arg-Phe-amide motif common in vertebrate Kps,
449 and exhibit a much lower identity with vertebrate Kp sequences. Thus, the experimental
450 evidence collected from functional interaction studies, between *A. japonicus* Kps and KpRs,
451 was not sufficient to support a definite relationship between the neuropeptide and the
452 receptor.

453 To address this issue, the cross interaction between vertebrate and *A. japonicus* Kp/KpR was
454 evaluated in this study. Our specificity analysis showed that human, frog, and zebrafish KPs,
455 hKiss1-10, XtKiss1b-10, and zfKiss1-10 and zfKiss2-10, were potent in activating both
456 AjKissR1 and AjKissR2, while the human neuropeptide S (hNPS, as a negative control)
457 showed no potency for the activation to AjKissR1 nor AjKissR2. Likewise, neuropeptides
458 AjKiss1a and AjKiss1b could potentiate Ca²⁺ signaling by binding the human Kp receptor
459 hKiss1R and zebrafish Kp receptors zfKiss1Ra/b, similar to the corresponding active
460 decapeptides. This, to our knowledge, is the first experimental data directly confirming the
461 connection between the Kp/KpR systems of vertebrates and *A. japonicus*, therefore proving
462 the existence of this neuropeptide system in non-chordate species. Considering the high

463 conservation of the neuropeptides in different echinoderms [4, 22], our finding that the Kp
464 signaling system exists in *A. japonicus* may be extend to other taxa in this phylum.

465 **Conserved $G_{\alpha q}$ /PLC/PKC/MAPK intracellular pathway mediated by *A. japonicus***

466 **Kp/KpR system provides insights into the evolution of Kp signaling**

467 It is well established that in mammals, Kiss1R is a typical $G_{\alpha q}$ -coupled receptor, triggering
468 PLC, intracellular Ca^{2+} mobilization, and the PKC signaling cascade in response to agonists
469 [16]. However, accumulating evidence shows that in teleosts, while both Kp receptors
470 preferentially activate the $G_{\alpha q}$ -dependent PKC pathway, one of them is also capable of
471 triggering the $G_{\alpha s}$ -dependent PKA cascade in response to Kp challenge [50, 52]. Using
472 CRE-Luc and SRE-Luc reporting assays, which helps discriminate between the AC/PKA and
473 PLC/PKC signaling pathways, an amphioxus Kp receptor was shown to trigger significant
474 PKC and not PKA signaling, when stimulated by two Kp-type peptides [19].

475 In this study, our data showed that upon synthetic peptide stimulation, both AjKissR1 and
476 AjKissR2 induced a rapid and transient rise of intracellular Ca^{2+} , in a dose-dependent manner,
477 via the $G_{\alpha q}$ -coupled signaling pathway. Further investigation of AjKissR1 and AjKissR2
478 mediated cell signaling indicated that AjKissR1 and AjKissR2 share similar intracellular
479 signaling pathways, via $G_{\alpha q}$ /PLC/PKC and ERK1/2 phosphorylation. Our results showed no
480 significant accumulation of cAMP, as detected by ELISA, indicating that $G_{\alpha s}$ -dependent PKA
481 signaling was not activated by the Kp receptors of *A. japonicus*. Since the $G_{\alpha q}$ -coupled PKC
482 signaling pathway, mediated by identified Kp systems, is conserved in all chordate species
483 and *A. japonicus*, and the $G_{\alpha s}$ -dependent PKA signaling was conserved in only a few teleost
484 Kp receptors (mainly from the KpR3 subfamily), we propose that $G_{\alpha q}$ -coupled signaling

485 activation originally evolved in this hypothalamic neuropeptide system.

486 **Reproductive and metabolic regulatory functions identified in *A. japonicus* revealed the**
487 **ancient physiological roles of the Kp system**

488 Diverse physiological functions of the Kp system have been reported in vertebrate species. In
489 mammals, it is widely established that the Kp signaling system is essential for HPG axis
490 regulation, leading to reproductive control, and the hypothalamic kisspeptin neurons have
491 been found to stimulate pituitary gonadotropin-releasing hormone neurons, which express the
492 kisspeptin receptor, providing a neural pathway of mammalian Kp neuronal system [56]. In
493 non-mammalian species, especially in teleosts, the reproductive function of the Kp system is
494 still controversial, considering the normal reproductive phenotypes observed in fishes in the
495 absence of Kps. A new theory has been proposed that the nonreproductive functions outside
496 HPG regulation, are the conserved roles of Kps in vertebrates [57, 58]. Here, we applied
497 multiple approaches to analyze the potential functions of the recently identified Kp in *A.*
498 *japonicus*, aiming to give some insights into the ancient physiological roles of the Kp system.
499 As described in this study, the expressional distribution of the *A. japonicus* Kp/KpR protein in
500 multiple tissues suggests the involvement of the Kp signaling system in both reproductive and
501 non-reproductive functions. Interestingly, the unequally expressed Kp/KpR protein levels in
502 gonads, comparatively high Kp precursor level in testis, and high KpR protein levels in ovary
503 demonstrated in our study, revealed differential functions of the Kp system in different
504 genders of sea cucumber. Further investigation from both *in vivo* and *in vitro* experiments
505 would indicate a role for the Kp signaling system in regulating gut function in sea cucumber.
506 Combining the feeding regulatory function of VP/OT-type neuropeptides characterized in

507 echinoderm [8] and the interaction between Kp and VP/OT neural systems [58-60], we
508 suggest that Kp regulation on VP/OT system may exist in echinoderms, requiring further
509 exploration on the possible interaction between these two systems and an evolutionarily
510 conserved function of the Kp system.

511 **Materials and Methods**

512 **Materials.** For cDNA cloning and gene expression analysis in various tissues, individuals of
513 the sea cucumber *A. japonicus* were collected from separate culture ponds in Qingdao
514 (Shandong, China, in 2016–2017). Each batch was acclimated in seawater aquaria (salinity
515 range: 32.21–34.13) for seven days and further dissected, sampled, and stored in liquid
516 nitrogen for future use or directly used for tissue culture. Individuals for *in vivo* experiments
517 (94 ± 4.3 g) were collected from the same culture pond in November 2017, kept in a 500 L
518 tank, and fed with a formulated diet (45% marine mud, 50% Sargasso, and 5% shrimp shell
519 powder) before chemicals were administered. After 15 days, sea cucumbers were randomly
520 assigned to different groups (10 individuals per group). AjKiss1b-10 was dissolved in PBS
521 and intraperitoneal injection of 100 μ L AjKiss1b-10 (concentration of 0.5 mg/mL diluted in
522 PBS) or PBS alone, was conducted once every two days, at noon. After 40 days (December
523 10, 2017 to January 18, 2018) of chemical administration, animals were dissected and the
524 respiratory tree, intestine, muscle, and anterior part tissues were taken as sample from five
525 individuals, for each group and stored in liquid nitrogen for future use. Coelom fluid was
526 collected and stored at -20 °C for E2 detection. This experiment was carried out on Xixuan
527 Fishery Technology Island without temperature or light control (sea water temperature 11.5–
528 7.0 °C). Individuals used in the *in vitro* experiments (89 ± 2.4 g) were collected from the same

529 culture pond in May 2017 and the respiratory tree, muscle, body wall, intestine, anterior part
530 (containing nerve ring), and ovary were dissected and further restored in $-20\text{ }^{\circ}\text{C}$ for western
531 blotting or washed with PBS three times, in aseptic conditions, for tissue culture and *in vitro*
532 experiments.

533 **Bioinformatic searches and tools.** The cDNA sequences were used to query known
534 sequences in GenBank using the blastx utility, BLASTX 2.8.0+
535 (<http://blast.ncbi.nlm.nih.gov/>). The cDNA sequence of *A. japonicus* Kp receptors or Kp
536 precursor was translated into the predicted amino acid sequence with DNAMAN 8.0.
537 Analysis of physicochemical properties of proteins was based on Protparam
538 (<http://www.expasy.org/tools/protparam.html>). Analysis of transmembrane regions in the
539 protein was achieved by TMHMM (<http://topcons.cbr.su.se/>). The deduced amino acid
540 sequences were aligned using ClustalW. Color align property was generated by the Sequence
541 Manipulation Suite (http://www.bioinformatics.org/sms2/color_align_prop.html). Signal
542 peptide was predicted by SignalP-5.0 Server (<http://www.cbs.dtu.dk/services/SignalP/>).
543 Phylogenetic tree construction was based on the Maximum Likelihood (ML) Method of
544 Molecular Evolutionary Genetics Analysis (MEGA 5.1). The bootstrap value was repeated 1,
545 000 times to obtain the confidence value for the analysis.

546 **Molecular Cloning and Plasmid Construction.** To construct the AjKissR1/2 fusion
547 expression plasmids, RT-PCR was performed using total RNA extracted from *A. japonicus*
548 ovaries, to synthesize template cDNA. PCR amplification for coding sequences of *AjKissR1/2*
549 was performed using specific primers, with restriction sites (Supplementary Table 2). The
550 corresponding PCR products were then cloned to pCMV-FLAG and pEGFP-N1 vectors,

551 respectively, using restriction enzymes and Rapid DNA Ligation Kit (Beyotime, China).
552 FLAG-hKiss1R plasmid was constructed using total synthesized DNA (Wuhan Transduction
553 Bio) with specific primers containing restriction sites (Supplementary Table 2). All constructs
554 were sequenced to verify the correct sequences, orientations, and reading frames.

555 **Cell culture and transfection.** HEK293 cells were cultured in DMEM (HyClone)
556 supplemented with 10% FBS, 100 U/mL penicillin, 100 mg/mL streptomycin and 4.0 mM
557 L-glutamine (Thermo Fisher Scientific) at 37 °C in a humidified incubator containing 5%
558 CO₂. The plasmid constructs were transfected into HEK293 cells by using X-tremeGENE HP
559 (Roche), according to the manufacturer's instructions. Two days after transfection, stably
560 expressing cells were selected by the addition of 800 mg/L G418.

561 **Intracellular calcium measurement.** The fluorescent Ca²⁺ indicator Fura-2/AM was used to
562 detect intracellular calcium flux [61]. Briefly, the AjKissR1 or AjKissR2 expressing HEK293
563 cells were washed twice with PBS and suspended at 5×10⁶ cells/mL in Hanks' balanced salt
564 solution. The cells were then loaded with 3.0 μM Fura-2/AM for 30 min and washed twice in
565 Hanks' solution. The cells were then stimulated with the indicated concentrations of different
566 predicted *A. japonicas* Kps or vertebrate Kps. Finally, intracellular calcium flux was
567 measured for 60 s, by the ratio of excitation wavelengths at 340 and 380 nm, using a
568 fluorescence spectrometer (Infinite 200 PRO, Tecan, Männedorf, Switzerland). All the
569 experiments for measuring Ca²⁺ mobilization were repeated independently at least thrice.

570 **Receptor localization and translocation assay, by confocal microscopy.** For the expression
571 and translocation analysis of receptors, HEK293 cells expressing AjKissR1/2-EGFP were
572 seeded onto glass coverslips in 12-well plates, coated with 0.1 mg/mL poly-L-lysine and

573 allowed to attach overnight under normal growth conditions [61]. The cells were washed three
574 times with PBS and further incubated with or without DAPI for several minutes. The
575 translocation of the receptor was measured with 1.0 μ M of various stimuli for 30 min. Cells
576 were washed three times with PBS and then fixed with 4% paraformaldehyde in PBS for 10
577 min at room temperature. Finally, the cells were mounted in mounting reagent
578 (DTT/PBS/glycerol,1:8:2) and visualized by fluorescence microscopy on a Zeiss laser
579 scanning confocal microscope, which was attached to a Zeiss Axiovert 200 microscope and
580 linked to a LSM5 computer system.

581 **PKC subtype recruitment assay by confocal microscopy**

582 Kisspeptin/GPR54 mediated PKC subtype recruitment assay in AjKissr1/2-expressing
583 HEK293 cells, was done after treatment with 1 μ M of different kisspeptins. HEK293 cells
584 co-transfected with FLAG-AjKissR1 or FLAG-AjKissR2 and various PKC-EGFP were
585 stimulated with AjKiss1b-10 (1 μ M) for the indicated periods and then examined by confocal
586 microscopy, for fusion protein localization and translocation assay.

587 **Antibodies.** The primary antibodies used for pERK1/2, ERK1/2, or β -tubulin detection were:
588 rabbit anti-phospho-ERK1/2(Thr²⁰²/Tyr²⁰⁴) antibody (1:2,000; Cell Signaling Technology),
589 rabbit anti-ERK1/2 antibody (1:2,000; Cell Signaling Technology), and beta-tubulin rabbit
590 monoclonal antibody (1:2,000; Beyotime). To examine the *A. japonicus* kisspeptin precursor
591 or AjKissR1 in various tissues of sea cucumber, AjKiss1b-10 or a peptide corresponding to
592 amino acids Ser¹⁵⁰~Trp¹⁷⁴ of AjKissR1, the second intracellular loop, was synthesized and
593 injected into two rabbits, respectively. The polyclonal antibodies, rabbit anti-AjKiss1b-10
594 (1:1,000) was prepared by ChinaPeptides and anti-AjKissR1 (1:1,000) was prepared by

595 Wuhan Transduction Bio. The secondary antibodies used were, HRP-conjugated goat
596 anti-rabbit IgG (Beyotime) and FITC-conjugated goat anti-rabbit IgG (Beyotime).

597 **Protein extraction and western blotting.** To examine the phosphorylation of ERK, cells that
598 expressed AjKissr1/2 or other GPR54s, were incubated for the indicated times with different
599 concentrations of kisspeptins [62]. Subsequently, cells were lysed with lysis buffer (Beyotime)
600 that contained protease inhibitor (Roche) at 4 °C for 30 min on a rocker and then scraped.
601 Proteins were then electrophoresed on a 10% SDS polyacrylamide gel and transferred to
602 PVDF membranes. Membranes were blocked with 5% skim milk, then probed with rabbit
603 anti-phospho-ERK1/2(Thr²⁰²/Tyr²⁰⁴) antibody (1:2,000; Cell Signaling Technology), followed
604 by detection using HRP-conjugated goat anti-rabbit IgG (Beyotime). Blots were stripped and
605 reprobed by using anti-ERK1/2 antibody (1:2,000; Cell Signaling Technology), as a control
606 for protein loading.

607 To detect AjKissR1 in different tissues of sea cucumber, the respiratory tree, intestine, muscle,
608 nerve ring, and ovary was sampled and homogenized with lysis buffer (Beyotime) that
609 contained protease inhibitor (Roche) at 4 °C. Comparable concentrations of proteins were
610 then electrophoresed on a 10% SDS polyacrylamide gel and transferred to PVDF membranes.
611 Membranes were blocked with 5% skim milk, then probed with rabbit anti-AjKissR1 serum
612 (1:1,000), followed by detection using HRP-conjugated goat anti-rabbit IgG (Beyotime).
613 Samples were probed in parallel with anti-tubulin antibody (Beyotime), as control for protein
614 loading.

615 Immunoreactive bands were detected with an enhanced chemiluminescent substrate
616 (Beyotime), and the membrane was scanned by using a Tanon 5200 Chemiluminescent

617 Imaging System (Tanon Science & Technology, Shanghai, China).

618 **Ligand competition binding assay.** A fluorescence-activated cell sorter (FACS) was used to
619 detect the binding ability of Kps with AjKissR1 or AjKissR2. HEK293 cells, expressing
620 Flag-AjKissR1 or Flag-AjKissR2, were washed with PBS that contained 0.2% bovine serum
621 albumin (FACS buffer). We designed and synthesized N-terminal FITC-labeled AjKiss1a
622 peptides (Supplementary table 1). Different Kps were diluted in the FACS buffer to different
623 concentrations, then added to cells that were incubated on ice for 60–90 min. Cells were
624 washed thrice with the FACS buffer and re-suspended in the FACS buffer with 1%
625 paraformaldehyde, for 15 min. The binding activity of indicated Kp peptides with AjKissR1
626 or AjKissR2 was determined by measuring the fluorescence of FITC and was presented as a
627 percentage of total binding.

628 **Immunofluorescence assay on paraffin-embedded tissue sections.** Paraffin sections were
629 baked at 60 °C for 2–4 h and placed in xylene for 15 minutes, twice. The slides were washed
630 twice in 100% ethanol for 10 min each, then in 95% ethanol for 10 min, 85% ethanol for 5
631 min, 70% ethanol for 5 min, 50% ethanol for 5 min followed by washing with dH₂O for 5 min,
632 and finally washing with PBS for 5 min. Antigen unmasking was performed in sodium citrate
633 buffer, pH 6, for 10 min at 97 °C and then cooling to room temperature. Endogenous
634 peroxidases were blocked by 10-min incubation in 3.0% hydrogen peroxide. Nonspecific
635 antigens were blocked by a 60-min incubation in 0.3% bovine serum albumin (BSA) in TBST.
636 Slides were incubated with primary antibodies overnight after removing the blocking solution,
637 followed by 2 h incubation with Fluorescein Isothiocyanate (FITC)-conjugated secondary
638 antibodies (FITC-labeled goat anti-rabbit IgG (H+L), Beyotime). Slides was washed with

639 dH₂O, mounted with antifade mounting medium (Beyotime), and imaged by confocal
640 microscopy.

641 **Real-time quantitative PCR (qRT-PCR).** For qRT-PCR, *β-actin* (ACTB) and *β-tubulin*
642 (TUBB) were chosen as the internal control (housekeeping) genes and gene-specific primers
643 were designed based on the ORF sequences [39, 63]. Specific qRT-PCR primers for
644 *AjKissR1/2* and *AjKiss1* were designed based on CDS (Supplementary Table 3). The primers
645 were tested to ensure amplification of single discrete bands, with no primer-dimers. qRT-PCR
646 assays were carried out using the SYBR PrimeScript™ RT reagent Kit (TaKaRa, Kusatsu,
647 Japan) following manufacturer's instructions and ABI 7500 Software v2.0.6 (Applied
648 Biosystems, UK). The relative level of gene expression was calculated using the 2^{-ΔC_t} method
649 and data was normalized by geometric averaging of the internal control genes [64, 65].

650 **Tissue culture.** For *in vitro* experiments, the ovary and respiratory tree tissues were cut into
651 small pieces of approximately 1 mm³ and cultured in Leibovitz L-15 medium (HyClone)
652 supplemented with 12.0 g/L NaCl, 0.32 g/L KCl, 0.36 g/L CaCl₂, 0.6 g/L Na₂SO₄, 2.4 g/L
653 MgCl₂, 0.6 g/L glucose, 1.5 U/mL penicillin, and 1.5 U/mL streptomycin, at 18 °C in a
654 humidified incubator.

655 **Radioimmunoassay.** Levels of estradiol (E2) in coelomic fluid or culture medium were
656 measured using the Iodine (¹²⁵I) method [66]. In brief, estradiol levels were measured using
657 Iodine (¹²⁵I) radioimmunoassay kits (Beijing North Institute of Biotechnology, Beijing, China),
658 according to the manufacturer's protocol. The binding rate is highly specific with an
659 extremely low cross-reactivity to other naturally occurring steroids, which was less than 0.1%
660 to most circulating steroids.

661 **Data Statistics.** Statistical analysis was done with GraphPad Prism (version 7.0). Statistical
662 significance was determined using the Student's t test and analysis of variance (ANOVA).
663 Probability values that were less than or equal to 0.05 were considered significant (*P < 0.05,
664 **P < 0.01), and all error bars represent standard error of the mean (SEM). All experimental
665 data were gathered from at least 3 independent experiments showing similar results.

666

667 **Acknowledgements**

668 The authors of this paper would like to thank Prof. Igor Yu. Dolmatov from National
669 Scientific Center of Marine Biology-Russian Academy of Sciences for his assistance on
670 histomorphological analysis and Prof. Dongdong Xu for his technical assistance and
671 equipment usage. This work was supported by the National Science Foundation of China
672 (Nos. 41876154, 41406137 and 41606150).

673

674 **Additional information**

675 **Competing interests:** The authors declare no competing financial interests.

676

677 **Author contributions:**

678 T.W. and N.Z. conceived and coordinated the study. T.W., J.Y., N.Z. and S.G. wrote the main
679 manuscript text, T.W. and X.C. prepared figures 1, 6 and 7, supplementary tables and related
680 supplementary figures, Z.C. and Z.S. prepared figures 2–5, and related supplementary figures.
681 T.W., J.Y., and N.Z. designed the experiments, Z.C., Z.S., Z.Y., K.X., X.X., Q.Y., Y.S., X.C.,
682 W.W and Y.T. performed the experiments. T.W., Z.C., Z.S. and N.Z. analyzed the results. L.S.,

683 L.Z, S.G. and N.Z. provided technical assistance and expert advice on English writing. All

684 authors reviewed the results and approved the final version of the manuscript.

685

686 **Data availability**

687 All the data needed to evaluate the conclusions of the paper are present in the paper and the

688 supplementary information files. All relevant data are available within source data files or

689 from the authors upon reasonable request.

690

691 References

- 692 1. Arendt D, Tosches MA, Marlow H. From nerve net to nerve ring, nerve cord and brain--evolution
693 of the nervous system. *Nat Rev Neurosci.* 2016;17(1):61-72. Epub 2015/12/18. doi:
694 10.1038/nrn.2015.15. PubMed PMID: 26675821.
- 695 2. Tessmar-Raible K. The evolution of neurosecretory centers in bilaterian forebrains: insights from
696 protostomes. *Semin Cell Dev Biol.* 2007;18(4):492-501. Epub 2007/06/20. doi:
697 10.1016/j.semcdb.2007.04.007. PubMed PMID: 17576082.
- 698 3. Tessmar-Raible K, Raible F, Christodoulou F, Guy K, Rembold M, Hausen H, Arendt D.
699 Conserved sensory-neurosecretory cell types in annelid and fish forebrain: insights into hypothalamus
700 evolution. *Cell.* 2007;129(7):1389-400. Epub 2007/07/03. doi: 10.1016/j.cell.2007.04.041. PubMed
701 PMID: 17604726.
- 702 4. Zandawala M, Moghul I, Yanez Guerra LA, Delroisse J, Abylkassimova N, Hugall AF, O'Hara TD.
703 Discovery of novel representatives of bilaterian neuropeptide families and reconstruction of
704 neuropeptide precursor evolution in ophiuroid echinoderms. *Open Biol.* 2017;7(9). Epub 2017/09/08.
705 doi: 10.1098/rsob.170129. PubMed PMID: 28878039; PubMed Central PMCID: PMC5627052.
- 706 5. Bakos J, Zatkova M, Bacova Z, Ostatnikova D. The Role of Hypothalamic Neuropeptides in
707 Neurogenesis and Neuritogenesis. *Neural Plast.* 2016;2016:3276383. Epub 2016/02/18. doi:
708 10.1155/2016/3276383. PubMed PMID: 26881105; PubMed Central PMCID: PMC4737468.
- 709 6. Burbidge S, Stewart I, Placzek M. Development of the Neuroendocrine Hypothalamus. *Compr*
710 *Physiol.* 2016;6(2):623-43. Epub 2016/04/12. doi: 10.1002/cphy.c150023. PubMed PMID: 27065164.
- 711 7. Hartenstein V. The neuroendocrine system of invertebrates: a developmental and evolutionary
712 perspective. *J Endocrinol.* 2006;190(3):555-70. Epub 2006/09/28. doi: 10.1677/joe.1.06964. PubMed
713 PMID: 17003257.
- 714 8. Odekunle EA, Semmens DC, Martynyuk N, Tinoco AB, Garewal AK, Patel RR, Blowes LM,
715 Zandawala M, Delroisse J, Slade SE, Scrivens JH, Egertová M, Elphick MR. Ancient role of
716 vasopressin/oxytocin-type neuropeptides as regulators of feeding revealed in an echinoderm. *BMC*
717 *Biol.* 2019;17(1).
- 718 9. Roseweir AK, Millar RP. The role of kisspeptin in the control of gonadotrophin secretion. *Hum*
719 *Reprod Update.* 2009;15(2):203-12. Epub 2008/12/26. doi: 10.1093/humupd/dmn058. PubMed PMID:
720 19109311.
- 721 10. Uenoyama Y, Pheng V, Tsukamura H, Maeda KI. The roles of kisspeptin revisited: inside and
722 outside the hypothalamus. *J Reprod Dev.* 2016;62(6):537-45. Epub 2016/08/02. doi:
723 10.1262/jrd.2016-083. PubMed PMID: 27478063; PubMed Central PMCID: PMC5177970.
- 724 11. Dhillon WS, Chaudhri OB, Patterson M, Thompson EL, Murphy KG, Badman MK, McGowan BM,
725 Amber V, Patel S, Ghatei MA, Bloom SR. Kisspeptin-54 stimulates the hypothalamic-pituitary gonadal
726 axis in human males. *J Clin Endocr Metab.* 2005;90(12):6609-15. doi: 10.1210/jc.2005-1468. PubMed
727 PMID: ISI:000233754000042.
- 728 12. Dhillon WS, Chaudhri OB, Thompson EL, Murphy KG, Patterson M, Ramachandran R, Nijher GK,
729 Amber V, Kokkinos A, Donaldson M, Ghatei MA, Bloom SR. Kisspeptin-54 stimulates gonadotropin
730 release most potently during the Preovulatory phase of the menstrual cycle in women. *J Clin Endocr*
731 *Metab.* 2007;92(10):3958-66. doi: 10.1210/jc.2007-1116. PubMed PMID: ISI:000250148400030.
- 732 13. Gottsch ML, Cunningham MJ, Smith JT, Popa SM, Acohido BV, Crowley WF, Seminara S,
733 Clifton DK, Steiner RA. A role for kisspeptins in the regulation of gonadotropin secretion in the mouse.

- 734 Endocrinology. 2004;145(9):4073-7. doi: 10.1210/en.2004-0431. PubMed PMID:
735 ISI:000223401600013.
- 736 14. Albers-Wolthers KH, de Gier J, Kooistra HS, Rutten VP, van Kooten PJ, de Graaf JJ, Leegwater
737 PA, Millar RP, Schaefer-Okkens AC. Identification of a novel kisspeptin with high gonadotrophin
738 stimulatory activity in the dog. Neuroendocrinology. 2014;99(3-4):178-89. Epub 2014/06/07. doi:
739 10.1159/000364877. PubMed PMID: 24902774.
- 740 15. Muir AI, Chamberlain L, Elshourbagy NA, Michalovich D, Moore DJ, Calamari A, Szekeres PG,
741 Sarau HM, Chambers JK, Murdock P, Steplewski K, Shabon U, Miller JE, Middleton SE, Darker JG,
742 Larminie CG, Wilson S, Bergsma DJ, Emson P, Faull R, Philpott KL, Harrison DC. AXOR12, a novel
743 human G protein-coupled receptor, activated by the peptide KiSS-1. J Biol Chem.
744 2001;276(31):28969-75. Epub 2001/06/02. doi: 10.1074/jbc.M102743200. PubMed PMID: 11387329.
- 745 16. Kirby HR, Maguire JJ, Colledge WH, Davenport AP. International Union of Basic and Clinical
746 Pharmacology. LXXVII. Kisspeptin Receptor Nomenclature, Distribution, and Function. Pharmacol
747 Rev. 2010;62(4):565-78. doi: 10.1124/pr.110.002774. PubMed PMID: ISI:000284214900001.
- 748 17. Javed Z, Qamar U, Sathyapalan T. The role of kisspeptin signalling in the
749 hypothalamic-pituitary-gonadal axis--current perspective. Endokrynol Pol. 2015;66(6):534-47. Epub
750 2015/12/15. doi: 10.5603/EP.2015.0066. PubMed PMID: 26662653.
- 751 18. Pasquier J, Kamech N, Lafont AG, Vaudry H, Rousseau K, Dufour S. Molecular evolution of
752 GPCRs: Kisspeptin/kisspeptin receptors. J Mol Endocrinol. 2014;52(3):T101-17. Epub 2014/03/01. doi:
753 10.1530/JME-13-0224. PubMed PMID: 24577719.
- 754 19. Wang P, Wang M, Ji G, Yang S, Zhang S, Liu Z. Demonstration of a Functional
755 Kisspeptin/Kisspeptin Receptor System in Amphioxus With Implications for Origin of Neuroendocrine
756 Regulation. Endocrinology. 2017;158(5):1461-73. Epub 2017/03/23. doi: 10.1210/en.2016-1848.
757 PubMed PMID: 28324048.
- 758 20. Mirabeau O, Joly JS. Molecular evolution of peptidergic signaling systems in bilaterians. Proc
759 Natl Acad Sci U S A. 2013;110(22):E2028-37. Epub 2013/05/15. doi: 10.1073/pnas.1219956110.
760 PubMed PMID: 23671109; PubMed Central PMCID: PMC3670399.
- 761 21. Elphick MR, Mirabeau O. The evolution and variety of RFamide-type neuropeptides: insights
762 from deuterostomian invertebrates. Front Endocrinol. 2014;5. doi: Artn 9310.3389/Fendo.2014.00093.
763 PubMed PMID: ISI:000209749800093.
- 764 22. Semmens DC, Elphick MR. The evolution of neuropeptide signalling: insights from echinoderms.
765 Brief Funct Genomics. 2017;16(5):288-98. Epub 2017/04/27. doi: 10.1093/bfpg/elx005. PubMed
766 PMID: 28444138.
- 767 23. Suwansa-ard S, Chaiyamon A, Talarovicova A, Tinikul R, Tinikul Y, Poomtong T, Elphick MR,
768 Cummins SF, Sobhon P. Transcriptomic discovery and comparative analysis of neuropeptide precursors
769 in sea cucumbers (Holothuroidea). Peptides. 2018;99:231-40. doi: 10.1016/j.peptides.2017.10.008.
770 PubMed PMID: ISI:000419525600029.
- 771 24. Semmens DC, Mirabeau O, Moghul I, Pancholi MR, Wurm Y, Elphick MR. Transcriptomic
772 identification of starfish neuropeptide precursors yields new insights into neuropeptide evolution. Open
773 Biol. 2016;6(2). doi: Artn 150224 10.1098/Rsob.150224. PubMed PMID: ISI:000371256100006.
- 774 25. Chen M, Talarovicova A, Zheng Y, Storey KB, Elphick MR. Neuropeptide precursors and
775 neuropeptides in the sea cucumber *Apostichopus japonicus*: a genomic, transcriptomic and proteomic
776 analysis. Sci Rep. 2019;9(1):8829. Epub 2019/06/22. doi: 10.1038/s41598-019-45271-3. PubMed
777 PMID: 31222106; PubMed Central PMCID: PMC6586643.

- 778 26. Purcell SW, Samyn Y, Conand C. Commercially important sea cucumbers of the world. *FAO*
779 *Species Catalogue for Fishery Purposes*. 2012;6:86-8.
- 780 27. Zhang XJ, Sun LN, Yuan JB, Sun YM, Gao Y, Zhang LB, Li SH, Dai H, Hamel JH, Liu CZ, Yu Y,
781 Liu SL, Lin WC, Guo KM, Jin SJ, Xu P, Storey KB, Huan P, Zhang T, Zhou Y, Zhang JQ, Lin CG, Li
782 XN, Xing LL, Huo D, Sun MZ, Wang L, Mercier A, Li FH, Yang HS, Xiang JH. The sea cucumber
783 genome provides insights into morphological evolution and visceral regeneration. *PLoS Biol*.
784 2017;15(10). doi: ARTN e2003790 10.1371/journal.pbio.2003790. PubMed PMID:
785 ISI:000414060400012.
- 786 28. Ukena K, Osugi T, Leprince J, Vaudry H, Tsutsui K. Molecular evolution of GPCRs:
787 26Rfa/GPR103. *J Mol Endocrinol*. 2014;52(3):T119-31. Epub 2014/02/18. doi: 10.1530/JME-13-0207.
788 PubMed PMID: 24532655.
- 789 29. Simakov O, Kawashima T, Marletaz F, Jenkins J, Koyanagi R, Mitros T, Hisata K, Bredeson J,
790 Shoguchi E, Gyoja F, Yue JX, Chen YC, Freeman RM, Sasaki A, Hikosaka-Katayama T, Sato A, Fujie
791 M, Baughman KW, Levine J, Gonzalez P, Cameron C, Fritzenwanker JH, Pani AM, Goto H, Kanda M,
792 Arakaki N, Yamasaki S, Qu J, Cree A, Ding Y, Dinh HH, Dugan S, Holder M, Jhangiani SN, Kovar CL,
793 Lee SL, Lewis LR, Morton D, Nazareth LV, Okwuonu G, Santibanez J, Chen R, Richards S, Muzny
794 DM, Gillis A, Peshkin L, Wu M, Humphreys T, Su YH, Putnam NH, Schmutz J, Fujiyama A, Yu JK,
795 Tagawa K, Worley KC, Gibbs RA, Kirschner MW, Lowe CJ, Satoh N, Rokhsar DS, Gerhart J.
796 Hemichordate genomes and deuterostome origins. *Nature*. 2015;527(7579):459-+. doi:
797 10.1038/nature16150. PubMed PMID: ISI:000365352500036.
- 798 30. Hall MR, Kocot KM, Baughman KW, Fernandez-Valverde SL, Gauthier MEA, Hatleberg WL,
799 Krishnan A, McDougall C, Motti CA, Shoguchi E, Wang TF, Xiang XY, Zhao M, Bose U, Shinzato
800 C, Hisata K, Fujie M, Kanda M, Cummins SF, Satoh N, Degnan SM, Degnan BM. The crown-of-thorns
801 starfish genome as a guide for biocontrol of this coral reef pest. *Nature*. 2017;544(7649):231-+. doi:
802 10.1038/nature22033. PubMed PMID: ISI:000398897900037.
- 803 31. Elphick MR. From gonadotropin-inhibitory hormone to SIFamides: Are echinoderm
804 SALMFamides the "missing link" in a bilaterian family of neuropeptides that regulate reproductive
805 processes? *Gen Comp Endocr*. 2013;193:229-33. doi: 10.1016/j.ygcen.2013.08.009. PubMed PMID:
806 ISI:000326427200027.
- 807 32. Shenoy SK, Lefkowitz RJ. Trafficking patterns of beta-arrestin and G protein-coupled receptors
808 determined by the kinetics of beta-arrestin deubiquitination. *J Biol Chem*. 2003;278(16):14498-506.
809 Epub 2003/02/08. doi: 10.1074/jbc.M209626200. PubMed PMID: 12574160.
- 810 33. Moore CA, Milano SK, Benovic JL. Regulation of receptor trafficking by GRKs and arrestins.
811 *Annu Rev Physiol*. 2007;69:451-82. Epub 2006/10/14. doi:
812 10.1146/annurev.physiol.69.022405.154712. PubMed PMID: 17037978.
- 813 34. Castano JP, Martinez-Fuentes AJ, Gutierrez-Pascual E, Vaudry H, Tena-Sempere M, Malagon
814 MM. Intracellular signaling pathways activated by kisspeptins through GPR54: do multiple signals
815 underlie function diversity? *Peptides*. 2009;30(1):10-5. Epub 2008/09/09. doi:
816 10.1016/j.peptides.2008.07.025. PubMed PMID: 18775460.
- 817 35. Lapadula D, Farias E, Randolph CE, Purwin T, McGrath D, Charpentier T, Zhang L, Wu S, Terai
818 M, Sato T, Tall GG, Zhou N, Wedegaertner P, Aplin AE, Aguirre-Ghiso J, Benovic JL. Effects of
819 Oncogenic Galphaq and Galpha11 Inhibition by FR900359 in Uveal Melanoma. *Mol Cancer Res*:
820 *MCR*. 2018. Epub 2018/12/21. doi: 10.1158/1541-7786.MCR-18-0574. PubMed PMID: 30567972.
- 821 36. Shen Z, Chen Y, Hong L, Cui Z, Yang H, He X, et al. BNGR-A25L and -A27 are two functional G

- 822 protein-coupled receptors for CAPA periviscerokinin neuropeptides in the silkworm *Bombyx mori*. J
823 Biol Chem. 2017;292(40):16554-70. Epub 2017/08/27. doi: 10.1074/jbc.M117.803445. PubMed PMID:
824 28842502; PubMed Central PMCID: PMC5633119.
- 825 37. Smiley S. Holothuroidea. Microscopic anatomy of invertebrates. 1994;14:401-71.
- 826 38. Wang T, Sun L, Chen M. Aestivation and Regeneration. Developments in Aquaculture and
827 Fisheries Science. 2015;39:177-209. doi: 10.1016/B978-0-12-799953-1.00011-8.
- 828 39. Xiang XW, Chen MY, Wu CW, Zhu AY, Yang JW, Lv ZM, Wang TM. Glycolytic regulation in
829 aestivation of the sea cucumber *Apostichopus japonicus*: evidence from metabolite quantification and
830 rate-limiting enzyme analyses. Mar Biol. 2016;163(8):1-12. doi: 10.1007/s00227-016-2936-5.
- 831 40. Popa SM, Clifton DK, Steiner RA. The role of kisspeptins and GPR54 in the neuroendocrine
832 regulation of reproduction. Annu Rev Physiol. 2008;70:213-38. doi:
833 10.1146/annurev.physiol.70.113006.100540. PubMed PMID: ISI:000254489400010.
- 834 41. Franssen D, Tena-Sempere M. The kisspeptin receptor: A key G-protein-coupled receptor in the
835 control of the reproductive axis. Best Pract Res Cl En. 2018;32(2):107-23. doi:
836 10.1016/j.beem.2018.01.005. PubMed PMID: ISI:000432235500004.
- 837 42. Ciaramella V, Della Corte CM, Ciardiello F, Morgillo F. Kisspeptin and Cancer: Molecular
838 Interaction, Biological Functions, and Future Perspectives. Front Endocrinol. 2018;9. doi: Artn 115
839 10.3389/Fendo.2018.00115. PubMed PMID: ISI:000428389600001.
- 840 43. Katugampola H, King PJ, Chatterjee S, Meso M, Duncan AJ, Achermann JC, Guasti L, Ghataore
841 L, Taylor NF, Allen R, Marlene S, Aquilina J, Abbara A, Jaysena CN, Dhillio WS, Dunkel L,
842 Sankilampi U, Storr HL. Kisspeptin Is a Novel Regulator of Human Fetal Adrenocortical Development
843 and Function: A Finding With Important Implications for the Human Fetoplacental Unit. J Clin Endocr
844 Metab. 2017;102(9):3349-59. doi: 10.1210/jc.2017-00763. PubMed PMID: ISI:000409352800028.
- 845 44. Jiang JH, Jin WD, Peng YL, He Z, Wei LJ, Li S, Wang XL, Chang M, Wang R. In vivo and vitro
846 characterization of the effects of kisspeptin-13, endogenous ligands for GPR54, on mouse
847 gastrointestinal motility. Eur J Pharmacol. 2017;794:216-23. doi: 10.1016/j.ejphar.2016.11.041.
848 PubMed PMID: ISI:000390647500027.
- 849 45. Song WJ, Mondal P, Wolfe A, Alonso LC, Stamateris R, Ong BWT, Lim OC, Yang KS, Radovick
850 S, Novaira HJ, Farber EA, Farber CR, Turner SD, Hussain MA. Glucagon Regulates Hepatic
851 Kisspeptin to Impair Insulin Secretion. Cell Metab. 2014;19(4):667-81. doi:
852 10.1016/j.cmet.2014.03.005. PubMed PMID: ISI:000333751600013.
- 853 46. Comminos AN, Wall MB, Demetriou L, Shah AJ, Clarke SA, Narayanaswamy S, Nesbitt A,
854 Izzi-Engbeaya C, Prague JK, Abbara A, Ratnasabapathy R, Salem V, Nijher GM, Jayasena CN, Tanner
855 M, Bassett P, Mehta A, Rabiner EA, Honigsperger C, Silva MR, Brandtzaeg OK, Lundanes E, Wilson
856 SR, Brown RC, Thomas SA, Bloom SR, Dhillio WS. Kisspeptin modulates sexual and emotional brain
857 processing in humans. J Clin Invest. 2017;127(2):709-19. doi: 10.1172/JCI89519. PubMed PMID:
858 ISI:000394164100030.
- 859 47. Huang H, Xiong Q, Wang N, Chen R, Ren H, Siwko S, Han H, Liu M, Qian M, Du B.
860 Kisspeptin/GPR54 signaling restricts antiviral innate immune response through regulating calcineurin
861 phosphatase activity. Sci Adv. 2018;4(8):eaas9784. Epub 2018/08/14. doi: 10.1126/sciadv.aas9784.
862 PubMed PMID: 30101190; PubMed Central PMCID: PMC6082648.
- 863 48. Jekely G. Global view of the evolution and diversity of metazoan neuropeptide signaling. Proc
864 Natl Acad Sci U S A. 2013;110(21):8702-7. Epub 2013/05/03. doi: 10.1073/pnas.1221833110. PubMed
865 PMID: 23637342; PubMed Central PMCID: PMC3666674.

- 866 49. Smith MK, Wang TF, Suwansa-ard S, Motti CA, Elizur A, Zhao M, Rowe ML, Hall MR, Elphick
867 MR, Cummins SF. The neuropeptidome of the Crown-of-Thorns Starfish, *Acanthaster planci*. J
868 Proteomics. 2017;165:61-8. doi: 10.1016/j.jprot.2017.05.026. PubMed PMID: ISI:000410470200007.
- 869 50. Biran J, Ben-Dor S, Levavi-Sivan B. Molecular identification and functional characterization of
870 the kisspeptin/kisspeptin receptor system in lower vertebrates. Biol Reprod. 2008;79(4):776-86. doi:
871 DOI 10.1095/biolreprod.107.066266. PubMed PMID: ISI:000259305300023.
- 872 51. Lee YR, Tsunekawa K, Moon MJ, Um HN, Hwang JI, Osugi T, Otaki N, Sunakawa Y, Kim K,
873 Vaudry H, Kwon HB, Seong JY, Tsutsui K. Molecular Evolution of Multiple Forms of Kisspeptins and
874 GPR54 Receptors in Vertebrates. Endocrinology. 2009;150(6):2837-46. doi: 10.1210/en.2008-1679.
875 PubMed PMID: ISI:000266256700047.
- 876 52. Ohga H, Fujinaga Y, Selvaraj S, Kitano H, Nyuji M, Yamaguchi A, Matsuyama M. Identification,
877 characterization, and expression profiles of two subtypes of kisspeptin receptors in a scombroid fish
878 (chub mackerel). Gen Comp Endocrinol. 193:130-40. Epub 2013/08/13. doi: S0016-6480(13)00320-1
879 [pii] 10.1016/j.ygcen.2013.07.016. PubMed PMID: 23932907.
- 880 53. Kotani M, Detheux M, Vandenbogaerde A, Communi D, Vanderwinden JM, Le Poul E, Brezillon
881 S, Tyldesley R, Suarea-Huerta N, Vandeput F, Blanpain C, Schiffmann SN, Vassart G, Parmentier M.
882 The metastasis suppressor gene KiSS-1 encodes kisspeptins, the natural ligands of the orphan G
883 protein-coupled receptor GPR54. J Biol Chem. 2001;276(37):34631-6. Epub 2001/07/18. doi:
884 10.1074/jbc.M104847200. PubMed PMID: 11457843.
- 885 54. Ohtaki T, Shintani Y, Honda S, Matsumoto H, Hori A, Kanehashi K, Terao Y, Kumano S, Takatsu
886 Y, Masuda Y, Ishibashi Y, Watanabe T, Asada M, Yamada T, Suenaga M, Kitada C, Usuki S, Kurokawa
887 T, Onda H, Nishimura O, Fujino M. Metastasis suppressor gene KiSS-1 encodes peptide ligand of a
888 G-protein-coupled receptor. Nature. 2001;411(6837):613-7. Epub 2001/06/01. doi: 10.1038/35079135.
889 PubMed PMID: 11385580.
- 890 55. Zmora N, Stubblefield J, Zulperi Z, Biran J, Levavi-Sivan B, Munoz-Cueto JA, Zohar Y.
891 Differential and Gonad Stage-Dependent Roles of Kisspeptin1 and Kisspeptin2 in Reproduction in the
892 Modern Teleosts, Morone Species. Biol Reprod. 2012;86(6). doi: ARTN 177
893 10.1095/biolreprod.111.097667. PubMed PMID: ISI:000306548000008.
- 894 56. Oakley AE, Clifton DK, Steiner RA. Kisspeptin signaling in the brain. Endocr Rev.
895 2009;30(6):713-43. Epub 2009/09/23. doi: 10.1210/er.2009-0005. PubMed PMID: 19770291; PubMed
896 Central PMCID: PMC2761114.
- 897 57. Tang HP, Liu Y, Luo DJ, Ogawa S, Yin YK, Li SS, Zhang Y, Hu W, Parhar IS, Lin HR, Liu XC,
898 Cheng CHK. The kiss/kissr Systems Are Dispensable for Zebrafish Reproduction: Evidence From
899 Gene Knockout Studies. Endocrinology. 2015;156(2):589-99. doi: 10.1210/en.2014-1204. PubMed
900 PMID: ISI:000353131800019.
- 901 58. Nakajo M, Kanda S, Karigo T, Takahashi A, Akazome Y, Uenoyama Y, Kobayashi M, Oka Y.
902 Evolutionally Conserved Function of Kisspeptin Neuronal System Is Nonreproductive Regulation as
903 Revealed by Nonmammalian Study. Endocrinology. 2018;159(1):163-83. Epub 2017/10/21. doi:
904 10.1210/en.2017-00808. PubMed PMID: 29053844.
- 905 59. Higo S, Honda S, Iijima N, Ozawa H. Mapping of Kisspeptin Receptor mRNA in the Whole Rat
906 Brain and its Co-Localisation with Oxytocin in the Paraventricular Nucleus. J Neuroendocrinol.
907 2016;28(4). Epub 2015/12/29. doi: 10.1111/jne.12356. PubMed PMID: 26709462.
- 908 60. Seymour AJ, Scott V, Augustine RA, Bouwer GT, Campbell RE, Brown CH. Development of an
909 excitatory kisspeptin projection to the oxytocin system in late pregnancy. J Physiol.

- 910 2017;595(3):825-38. Epub 2016/09/03. doi: 10.1113/JP273051. PubMed PMID: 27589336; PubMed
911 Central PMCID: PMC5285723.
- 912 61. Li G, Shi Y, Huang HS, Zhang YP, Wu KP, Luo JS, Sun Y, Lu JX, Benovic JL, Zhou NM.
913 Internalization of the Human Nicotinic Acid Receptor GPR109A Is Regulated by G(i), GRK2, and
914 Arrestin3. *J Biol Chem.* 2010;285(29):22605-18. doi: 10.1074/jbc.M109.087213. PubMed PMID:
915 ISI:000279702200071.
- 916 62. Shen ZF, Chen Y, Hong LJ, Cui ZT, Yang HP, He XB, Shi Y, Shi LG, Han F, Zhou NM.
917 BNGR-A25L and-A27 are two functional G protein-coupled receptors for CAPA periviscerokinin
918 neuropeptides in the silkworm *Bombyx mori*. *J Biol Chem.* 2017;292(40):16554-70. doi:
919 10.1074/jbc.M117.803445. PubMed PMID: ISI:000412414800017.
- 920 63. Zhu A, Chen M, Zhang X, Storey KB. Gene structure, expression, and DNA methylation
921 characteristics of sea cucumber cyclin B gene during aestivation. *Gene.* 2016. Epub 2016/09/08. doi:
922 10.1016/j.gene.2016.09.006. PubMed PMID: 27601256.
- 923 64. Livak KJ, Schmittgen TD. Analysis of relative gene expression data using real-time quantitative
924 PCR and the $2^{-\Delta\Delta C_T}$ method. *Methods.* 2001;25(4):402-8. doi: DOI
925 10.1006/meth.2001.1262. PubMed PMID: ISI:000173949500003.
- 926 65. Vandesompele J, De Preter K, Pattyn F, Poppe B, Van Roy N, De Paepe A, Spelem F. Accurate
927 normalization of real-time quantitative RT-PCR data by geometric averaging of multiple internal
928 control genes. *Genome Biol.* 2002;3(7):- . doi: Artn 0034.1 Doi 10.1186/Gb-2002-3-7-Research0034.
929 PubMed PMID: ISI:000207581200010.
- 930 66. Lu ZM, Liu W, Liu LQ, Wang TM, Shi HL, Ping HL, Shi CF, Yang JW, Wu CW. Cloning,
931 Characterization, and Expression Profile of Estrogen Receptor in Common Chinese Cuttlefish, *Sepiella*
932 *japonica*. *J Exp Zool A Ecol Genet Physiol.* 2016;325(3):181-93. Epub 2016/04/15. doi:
933 10.1002/jez.2011. PubMed PMID: 27076436.F

934

935

936 **Supplementary information**

937 Existence and functions of hypothalamic kisspeptin neuropeptide signaling system in
938 a non-chordate deuterostome species

939 This supplementary information section contains the following:

940 Supplementary figures:

- 941 ● Figure 1–figure supplement 1
- 942 ● Figure 1–figure supplement 2
- 943 ● Figure 1–figure supplement 3
- 944 ● Figure 1–figure supplement 4
- 945 ● Figure 4–figure supplement 1
- 946 ● Figure 5–figure supplement 1
- 947 ● Figure 6–figure supplement 1
- 948 ● Figure 6–figure supplement 2
- 949 ● Figure 6–figure supplement 3
- 950 ● Figure 6–figure supplement 4

951 Supplementary tables:

- 952 ● Supplementary table 1
- 953 ● Supplementary table 2
- 954 ● Supplementary table 3

955 Source data files:

- 956 ● Figure 2–source data
- 957 ● Figure 3–source data

- 958 ● Figure 4–source data
- 959 ● Figure 6–source data
- 960 ● Figure 6–figure supplement 3–source data
- 961 Raw data sets
- 962 ● Figure 1 raw data set 1
- 963 ● Figure 1 raw data set 2
- 964 ● Figure 1 raw data set 3
- 965 ● Figure 1–figure supplement 4–raw data set 1
- 966

```
1 AACTAGATCAAAGGAAGAGTCTTTTTACCTGCTGATAGTGGATTTTCGTTGCCAATTTACATTCTGATTGCATTTTTTTTTTCATGAGC
91 GACTTGAAAAGGAGAAAAAGTTCAATCATAAATCATTTGTGATCGTGTCTTGAGGAGGTGCTAACCCAGCTGGATCAAGGAGGCAAG
181 CTTTACGTGTAATCAAGGAAGGAGGCTCTATGCAATGGACAAAATAGTATTTCCCGATCCTACTGTCTGCTGTGGAACAGTGTTTAG
M D K I V F P I L L S L L C G T V F S
271 CGCATCACTAGCAGACACAAAATTTAAAAGATTACGAGGACAGTTAGACGACGCCAGAGAGGGTCTTAAACTTATCGCTGGATTATT
A S L A D T N L K D Y E D R L D D A R E R V L K L I A G L L
361 ATCTGATGATACGTACCAAGAGCAGTTTACTGGAGAACAAGACGAAGATGACCTTGCTGTAATAATACCAATTCTTAAAAATTTGCTCGC
S D D T Y Q E Q F T G E Q D E D D L A V N I P I L E N L L A
451 CGAGAACGACGGTGAAGATGTAATTGACGCTGACGATACGGCAGAGTTGATTTTGAATCCCTCTCTAATAATGGAAGACCCATAGACGA
E N D G E D V I D A D D T A E L I F E S L S N N G R P I D E
541 AAAGCGTGTGGGAGCTAGATTGCCTGGAAGCATCATGTGAAGATGTTGAACGCCGGGACGGCAACCGAATAGAAACGCCATTACAG
R R A G S L D C L E A S C E D V E R R G R Q P N R N A H Y R
631 GACGCTTCCATTCGGGAAAAGGTTACAAAGGCAAACCTTCTCGACTGTGAGGAATACGGGAAAATCAGCTGTGAAAAACAAGAACAGTC
T L P E G R R V Q R Q T F S T V R N T R K S A V K N K N K S
721 ACGTGCACGCCACCCCTTCTCCCTTCGGAAAATGAACAGTTGTTTTGAAGTATTGAGATTATCTTAAGCACTAGGCCACGTCAT
R A R P P L L P E G R *
811 TGTATTCATTACAGAAAGACTCTCACTCATTGTCTTTGCTCCTGTAATTTCAAGTAAATTCGTTTGCATATAATGTATATTTCTCTC
901 GTCCATTAATAGATACTAAAATGATTTGTATAAATTAAGTATGAAATTTGAGAATGGCTAATGACAGAAAAGAAAGTTAACAAAAATGAT
991 GTGCTTAATTTTGTCTAAGCTTGATAAATTTGGCTTGATTACACGTGAAGATAAATTTCTTAAAAGATCAAATCGTTATAATGGTAATA
1081 GTGCACACAAGTCTGAAATATATTGCACTTATTAGAACAAGACAATGAGTGATAGTGTGGTCTAATTATATAAATACATCGCGATCATT
1171 ATTAACCTGTACTTTCCGATTTGTTTCCCTCAATATTAACAACAATTAATATCTTAAACAATTTGCATTGCACTACATCAATATT
1261 TATCTTTTACAAACGGCAGAGACCTTAATTAACCTTTTGTGATGCCATGTGTTAAGAATGTACATGTTATTTCCGCAACTTCAAAT
1351 GTTTGTAGTCTTTCCGATTTCTTAAGATTTCTTGAAGTATGTTATATTATTACAAAACACAACCTCTTTGGCAAAGGTTTCGT
1441 ATAAGCATATCGACGTGAAAAGTAATAAATCTTGATCAATATCCCATCAATTTACGTACATTTACGTACACGATTAAATTTCACTTTC
1531 GCTGGTATTAGGAAAGCATCAATAATTGGAAGTCGGGTAATTTATGGATCAGCATTAAACATTTCAATTTCTAAATTCCTGTCTTTATCTG
1621 AAAATCACTTTATCCATGGGTTTCTCTCGAATATAAAAATAAATTAATAACTAATCTGTTGTCGAGAAATACATATAAACCGTGAATGTAGCCA
1711 CTGCTGCAAGGCTTATTTTACCTATTAATATTGTAATTTTGAAGTTCGTTCTCTGAACTGGAGAAGACCAATATTCACCTGGT
1801 ATGACATACGCAATCCGAGATCAAAATTACACCTGCCAAGCATAATTTGCTGTGGATTTCACAGACTTCTATCATTCAACTTCATATA
1891 TATTGTGCAAAATAACACTCCCAACACTTTCTTATTACAACAGTGTGGGAGAAATGAACATAATAGAAGATAATAGAACAGCCCCACCT
1981 GTATACATCACAACAACCTTGAATTTGCCACAATTTGACATTTGCACGAGTATTTCAAACGATCCTTGTCACTTCGTAGGAATACTTG
2071 GACGAATATCATAGAAAATAAGCAGTACTTGAAGTTGATATTTGATATGCGGAAAGACTAATGTGACATTGTTATTTAACATACTATTTCG
2161 TTCTTGTCTCTTGTTCGAATTCACGGTTCTTTTATTTTAAATTAACAAGAGGATTTCTCCAGCCTGTGGCGTCTGTATTACAGTC
2251 GATGTTTTCAACCTCCGTAATATCGATGCAATACCGTTCTGATGAATTTACTACCTTGGAAAACGGTGGGTGCATATGCTGGATAAA
2341 TTTGTAGTTAATAAATTAAGATTTACGTTAAACAATTTCAAGTATAAATATTGCAGAAAAGTACAGAACTATTACTTTGTGATCT
2431 CGCAAAGACTTTGATAAATACAGACGAGATAAAAAAAAAAAAAAAAAAAAA
```

967

968 **Figure 1–figure supplement 1.** Gene structure of *Apostichopus japonicus* kisspeptin (Kp) precursor.

969 The signal peptide, predicted by online SignalP-5.0 Server, is labeled in box with full lines; the

970 cleavage sites, predicted based on previously known consensus cleavage motifs by using the NeuroPred

971 program, are highlighted in red; glycine residues responsible for C-terminal amidation are highlighted

972 in green; cysteines paired in a disulfide-bonding structure are highlighted in light blue; the predicted

973 mature peptides with C-terminal amidation are noted underlined in black. The initiation codon (ATG)

974 and the termination codon (TGA) are shown in bold.

975

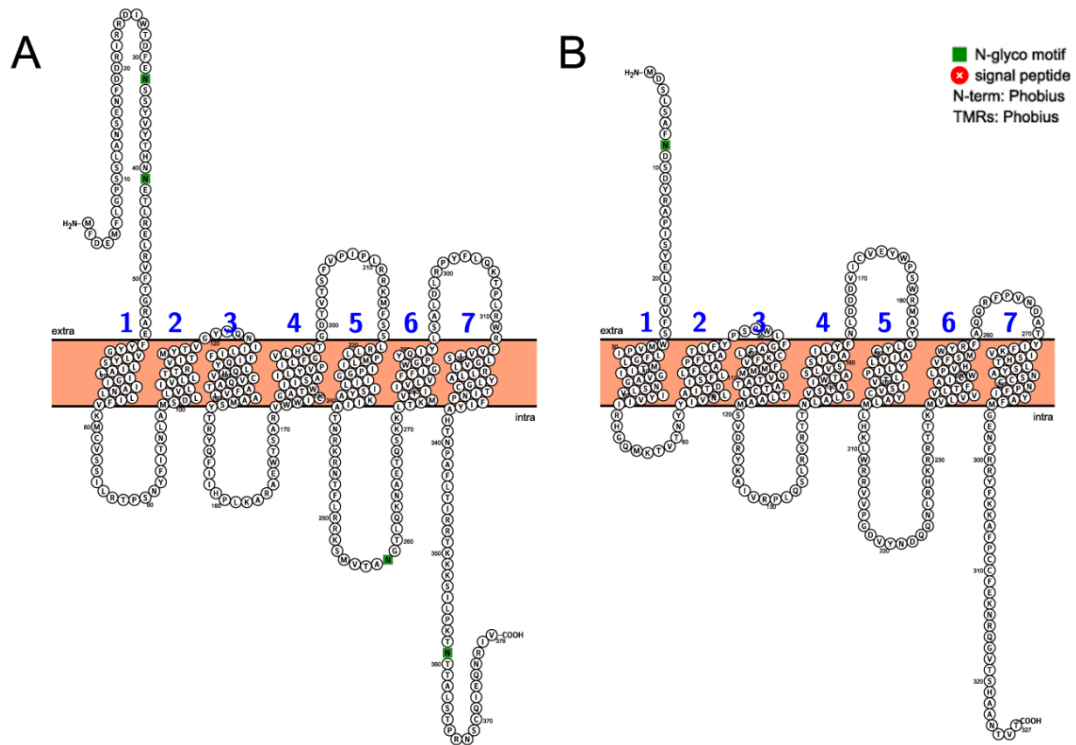
976

977

978

979

980



981

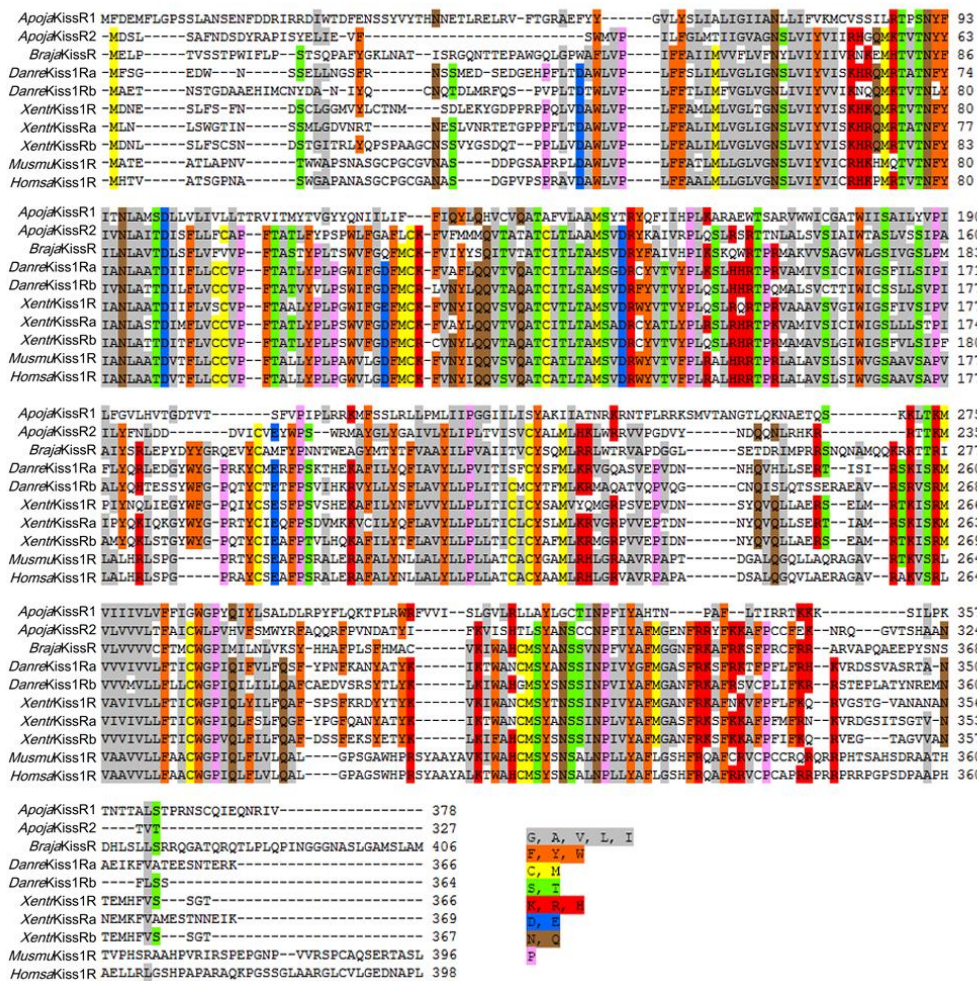
982 **Figure 1–figure supplement 2.** Sequence, topology and annotations of *Apostichopus japonicus*

983 kisspeptin receptors (A: AjKissR1, B: AjKissR2) visualized by a webservice of Protter.

984 <http://wlab.ethz.ch/protter/start/>.

985

986

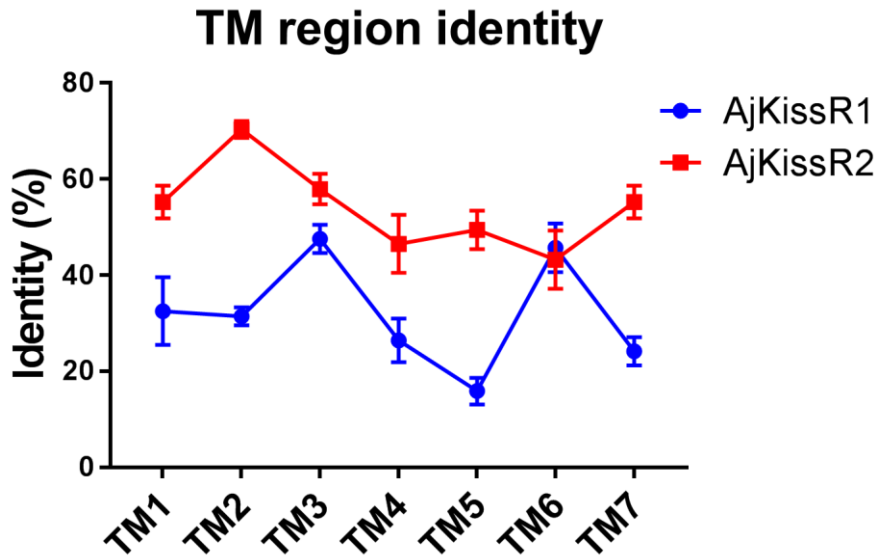


987

988 **Figure 1—figure supplement 3.** Alignment of the deduced *Apostichopus japonicus* kisspeptin receptor
 989 amino acid sequences with functionally characterized chordate GPR54 molecules from other species.
 990 Sequences of *Branchiostoma japonicum* kisspeptin (Kp) receptor (*BrajaKissR*), *Danio rerio* Kp
 991 receptors (*DanreKiss1Ra* NP_001099149.2 and *DanreKiss1Rb* NP_001104001.1), *Xenopus tropicalis*
 992 Kp receptors (*XentrKiss1R* NP_001163985.1, *XentrKissRa* NP_001165296.1 and *XentrKissRb*
 993 NP_001165295.1), *Mus musculus* Kp receptor (*MusmuKiss1R* NP_444474.1), and *Homo sapiens* Kp
 994 receptor (*HomsaKiss1R* NP_115940.2) were obtained from GenBank. Alignment was conducted using
 995 CLUSTAL W and the color align property was generated using Sequence Manipulation Suite online.
 996 Percentage of sequences that must agree for identity or similarity coloring was set as 60%.

997

998



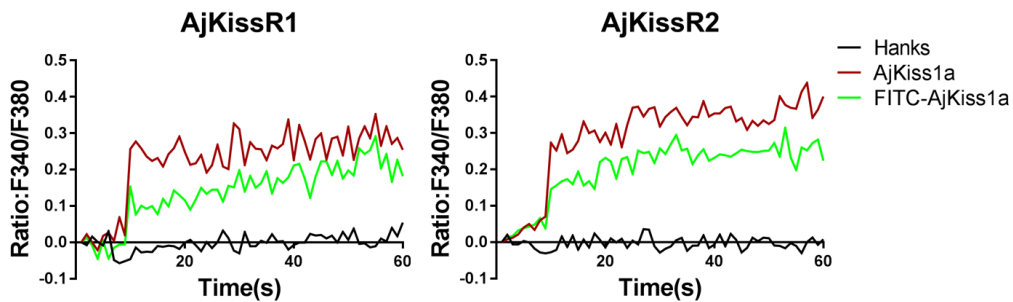
999

1000 **Figure 1–figure supplement 4.** Transmembrane region sequence similarity of *Apostichopus japonicus*
1001 kisspeptin receptors to vertebrate kisspeptin receptors. Detailed identities are listed in Figure 1–figure
1002 supplement 4 raw data set 1.

1003

1004

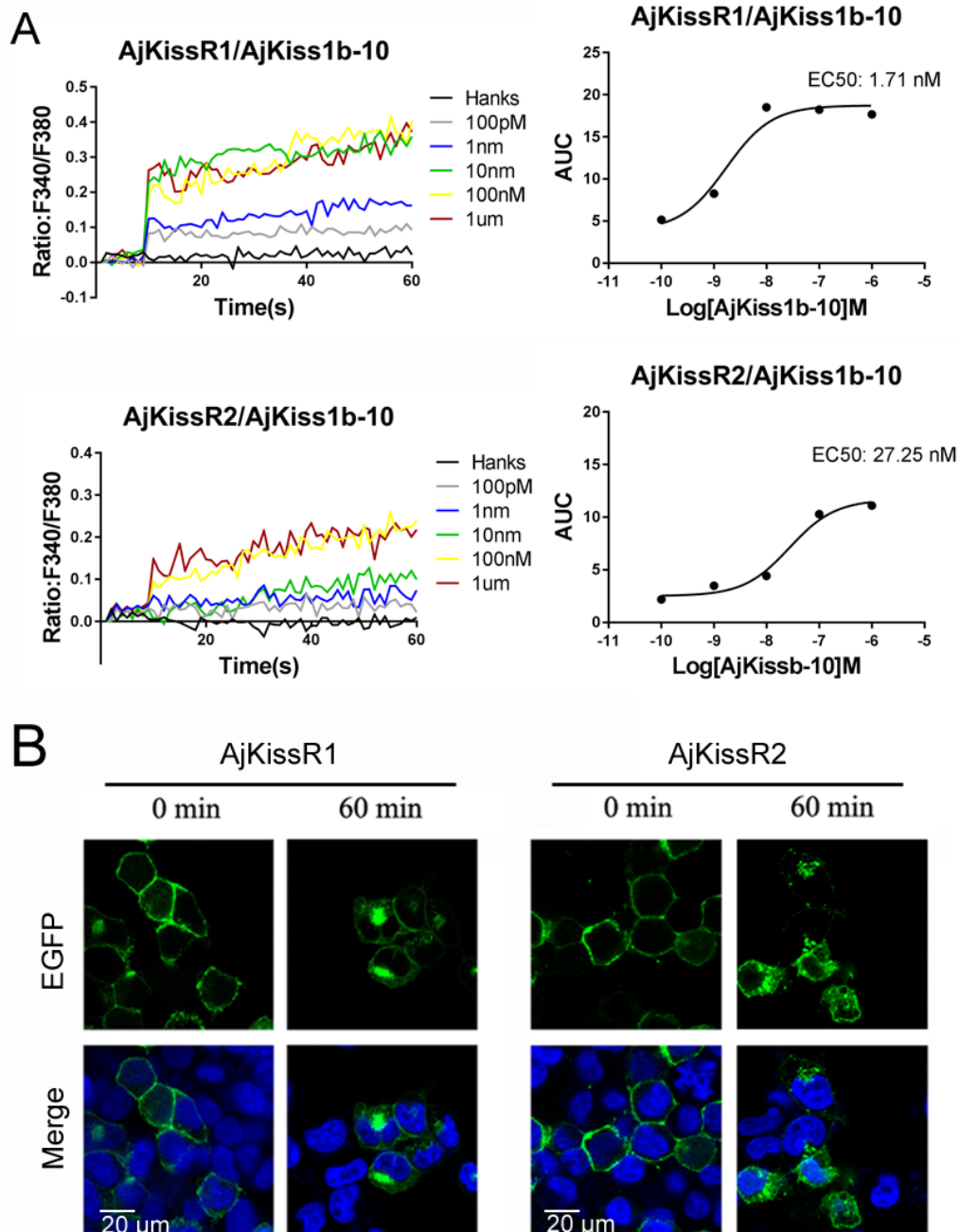
1005



1006

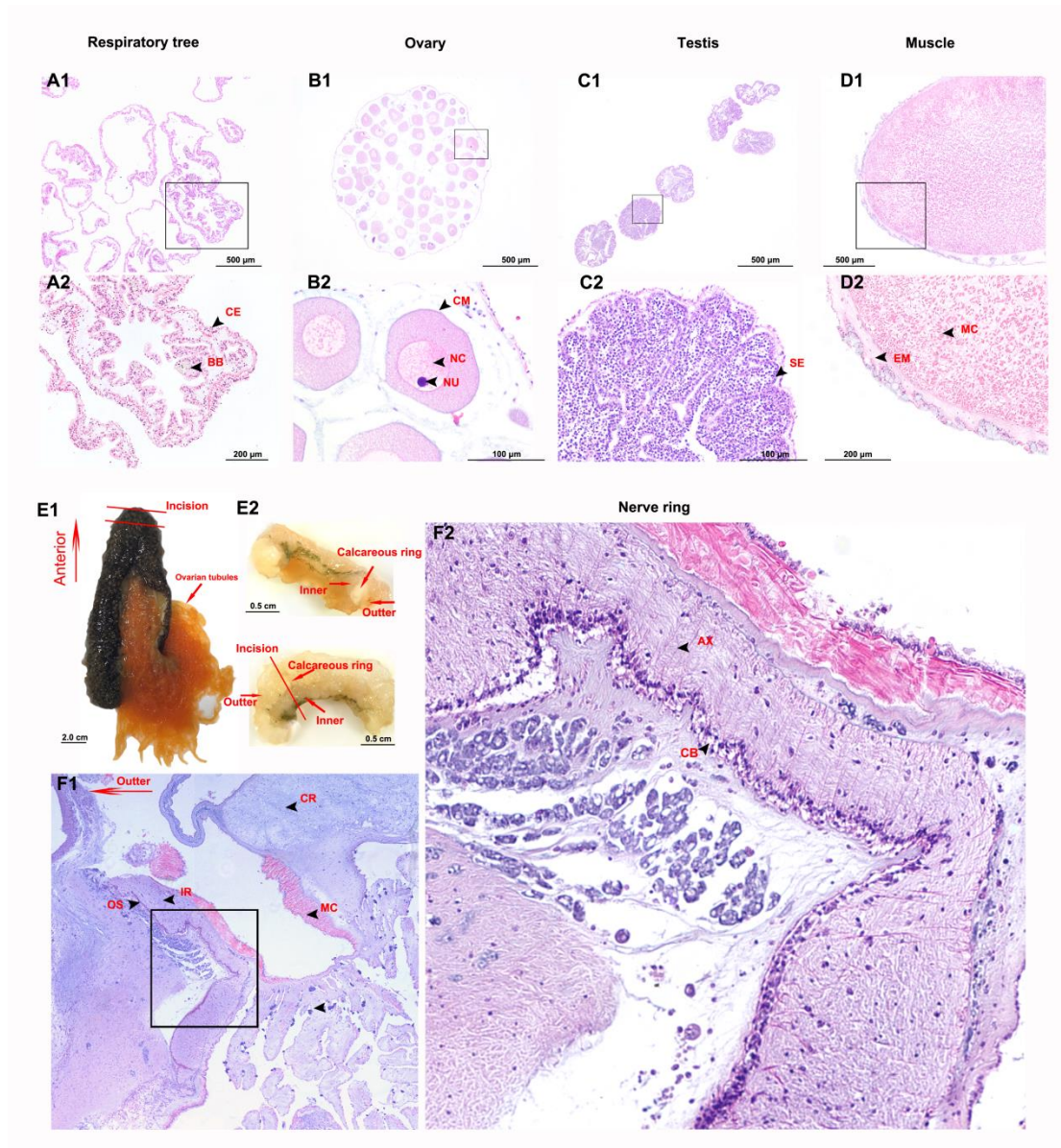
1007 **Figure 4–figure supplement 1.** Functional activity of FITC-AjKiss1a evaluated by intracellular Ca^{2+}
1008 mobilization detection. Intracellular Ca^{2+} mobilization in AjKissR1/2 expressing HEK293 cells was
1009 measured in response to 1.0 μ M stimuli using Fura-2/AM.

1010



1011

1012 **Figure 5—figure supplement 1.** Functional activity of AjKiss1b-10. **A.** Intracellular Ca^{2+} mobilization
 1013 in AjKissR1/2 expressing HEK293 cells was measured in response to AjKiss1b-10 with indicated
 1014 concentrations using Fura-2/AM. **B.** Internalization of overexpressed AjKissR1/2 initiated by 1.0 μ M
 1015 AjKiss1b-10 in AjKissR1-EGFP or AjKissR2-EGFP expressing HEK293 cells was determined by
 1016 confocal microscopy.



1017

1018 **Figure 6–figure supplement 1.** General morphology and histology of *Apostichopus japonicus* tissues.

1019 A-D. Light micrographs of H&E staining section of respiratory tree, ovary, testis and muscle. (CE)

1020 coelomic epithelium, (BB) brown body, (CM) cell membrane, (NC) nucleus of oocytes, (NU) nucleolus

1021 of oocytes, (SE) spermatogenic epithelium, (EM) epithelium of muscle, (MC) myocyte. E. Gross

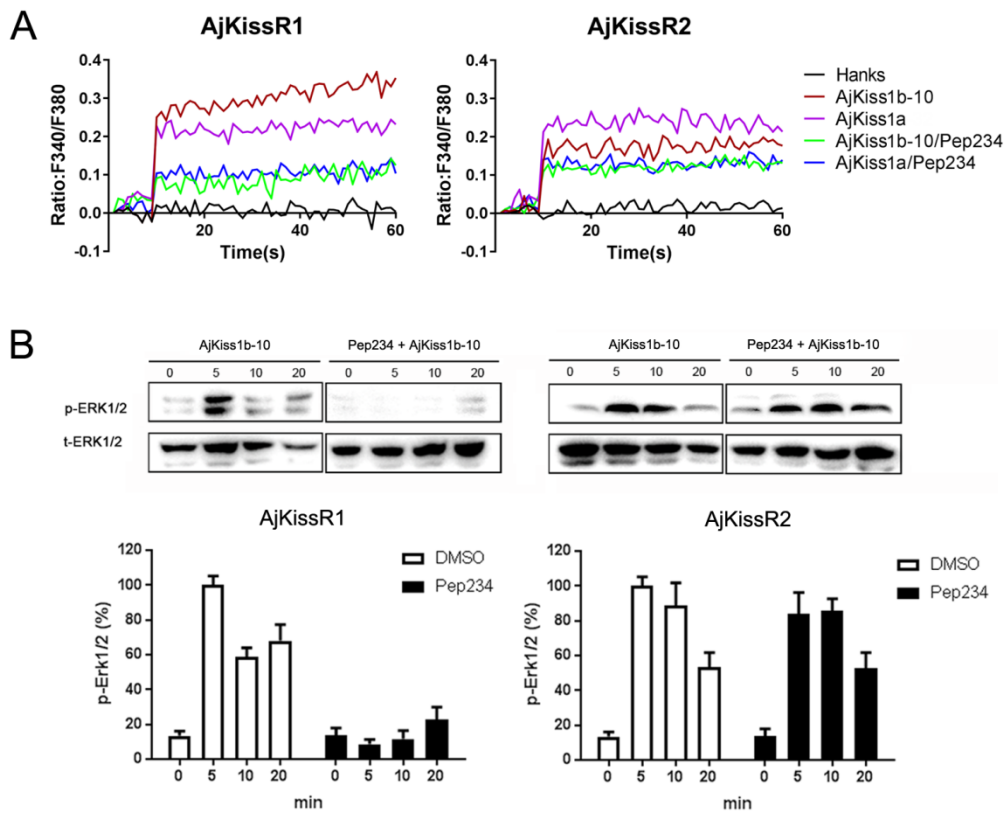
1022 anatomy of anterior part (ANP). F. Light micrographs of H&E staining section of ANP and histology of

1023 nerve ring (NR). (OS) outer surface, (IR) internal region, (CR) calcareous ring, (AX) axon of neuron,

1024 (CB) cell body of neuron.

1025

1026



1027

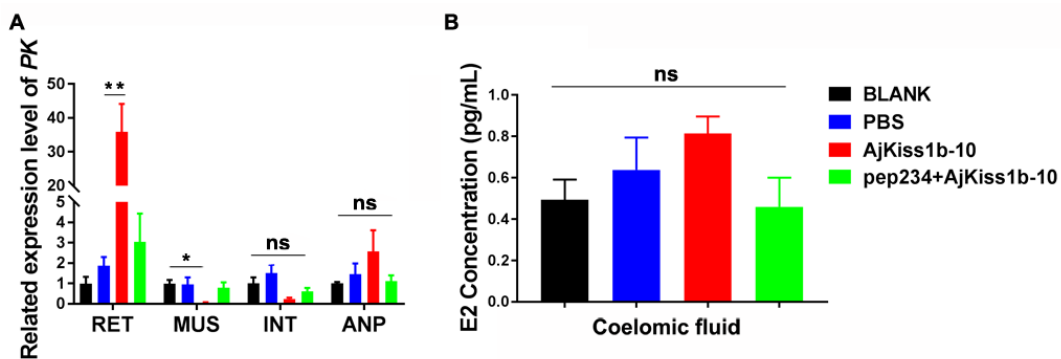
1028 **Figure 6–figure supplement 2.** Inhibitory effect of pep234 on AjKissR1 and AjKissR2 activation. **A.**

1029 Intracellular Ca^{2+} mobilization in AjKissR1 and AjKissR2 expressing HEK293 cells was measured in
1030 response to 100 nM AjKiss1a or AjKiss1b-10 pretreated with DMSO or KISS1 antagonist pep234 (1

1031 μ M). **B.** ERK1/2 phosphorylation activity of Kps and inhibitory effect of pep234 AjKissR1 and

1032 AjKissR2 expressing HEK293 cells. Samples were measured after 2 h of ligand administration with or

1033 without pretreatment of pep234. Error bars represent SEM for three independent experiments.



1034

1035 **Figure 6–figure supplement 3.** Functional activity of AjKiss1b-10 in *Apostichopus japonicus*. **A.**

1036 Gene expressional change of glycolytic enzyme gene *pyruvate kinase* (PK) in tissues of sea cucumbers

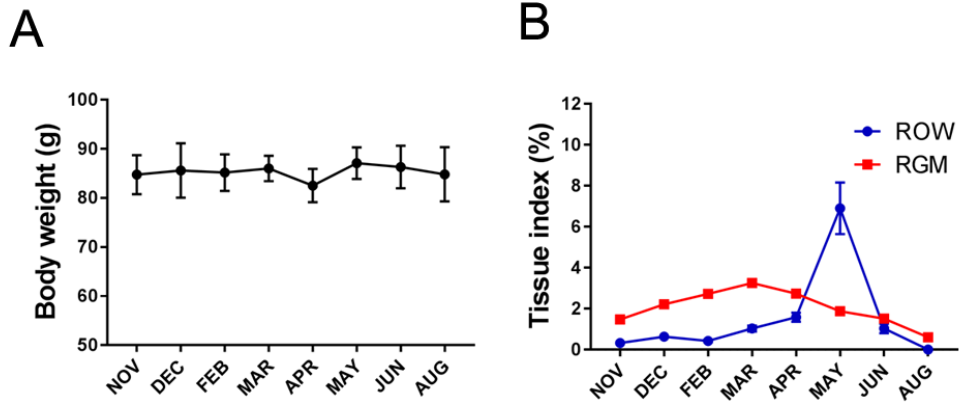
1037 responds to a 40-day administration of AjKiss1b-10. (RET) respiratory tree, (MUS) muscle, (INT)

1038 intestine, (ANP) anterior part of sea cucumber. **B.** E2 concentration in coelomic fluid of sea cucumbers

1039 did not significantly respond to AjKiss1b-10. Each symbol and vertical bar represents SEM (n=5). *

1040 indicates significant differences ($P < 0.05$), and ** indicates extremely significant differences ($P <$

1041 0.01), ANOVA, Tukey's multiple comparison test.



1042
1043 **Figure 6-figure supplement 4.** Mean body weight (A), relative gut mass (RGM), and relative ovary
1044 weight (ROW) (B) change over annual investigation. Each symbol and vertical bar represent SEM
1045 (n=5).

1046

1047

1048

1049

1050

1051

1052

1053

1054

1055

1056

1057

1058

1059 **Supplementary table 1.** Sequence information of synthetic neuropeptide used.

1060 Note: c< > indicates disulfide bond

Name	Sequence	Purity
AjKiss1a	AGSLDc<CLEASC>EDVERRGRQPN RNAHYRTLPF-NH2	>95%
FITC-AjKiss1a	FITC-AGSLDc<CLEASC>EDVERRGR QPNRNAHYRTLPF-NH2	>95%
AjKiss1a-15	GRQPNRNAHYRTLPF-NH2	>95%
AjKiss1a-10	AHYRTLPF-NH2	>95%
AjKiss1b	SAVKNKNSRARPPLLPF-NH2	>95%
AjKiss1b-10	SRARPPLLPF-NH2	>95%
hKISS1-10	YNWNSFGLRF-NH2	>95%
XtKISS3/KISS1b-10	YNVNSFGLRF-NH2	>95%
zfKISS1-10	YNLNSFGLRY-NH2	>95%
zfKISS2-10	FNYNPFGLRF-NH2	>95%

1061

1062 **Supplementary table 2.** Primers for plasmid construction

Plasmid name	Primer	Enzyme
AjKissR1-EGFP	FORWARD CGAATTCATGTTTGACGAAATGTTC	EcoR I
	REVERSE GTGGATCCCGAACGATACGATTCTGTTC	BamH I
FLAG-AjKissR1	FORWARD GGAATTCATGTTTGACGAAATGTTC	EcoR I
	REVERSE CGGGATCCTCAAACGATACGATTCTGTTC	BamH I
AjKissR2-EGFP	FORWARD CGAATTCATGGACAGCCTCTCAGC	EcoR I
	REVERSE CCGTCGACTGAGTTACAGTATTTGCTG	SaII
FLAG-AjKissR2	FORWARD CCAAGCTTGGATGGACAGCCTCTCAGCGTT	Hind III
	REVERSE CGGGATCCCGTGAGTTACAGTATTTGCTGCAT	Bam HI
FLAG-hKiss1R	FORWARD CCAAGCTTGGATGCACACCGTGGCTAC	Hind III
	REVERSE CGGGATCCTCAGAGAGGGGCGTTGTCCT	Bam HI

1063

1064 **Supplementary Table 3.** Primers for qPCR amplification

Gene name	Primer	Application
<i>AjKissR1</i>	FORWARD AGTGGACATCTGCAAGAGTATGG	Specific primer
	REVERSE CTTCCTGCGTAATGGTATCGGTA	
<i>AjKissR2</i>	FORWARD TCTCGTTGTTGTCTTGACGTTTG	Specific primer
	REVERSE TCGTCTGAAGTTTTCTCCCATGA	
<i>AjKiss1</i>	FORWARD CCTACTGTCATTGCTCTGTGGAAC	Specific primer
	REVERSE CAAGGTCATCTTCGTCTTGTCTC	
<i>β-tubulin</i>	FORWARD CACCACGTGGACTCAAATG	Internal control
	REVERSE GAAAGCCTTACGACGGAACA	
<i>β-actin</i>	FORWARD AAGGTTATGCTCTTCCTCACGC	Internal control
	REVERSE GATGTCACGGACGATTTACAG	

1065